Structural phase transition in $(GaAs)_{1-x}Ge_{2x}$ and $(GaP)_{1-x}Si_{2x}$ alloys: Test of the bulk thermodynamic description

Roberto Osório,* Sverre Froyen, and Alex Zunger
Solar Energy Research Institute, Golden, Colorado 80401
(Received 19 November 1990)

Nonisovalent $(A^{III}B^{V})_{1-x}C^{IV}_{2x}$ semiconductor alloys exhibit a transition as a function of composition between a phase with the zinc-blende symmetry (where the two fcc sublattices of the diamond lattice are unequally occupied by A^{III} and B^{V} atoms) and a phase with the diamond symmetry (where the two sublattices have equal occupations). Previous thermodynamic models of this transition have considered only nearest-neighbor interactions between *neutral* atoms. This approach ignores the important electrostatic interactions associated with electron transfer between the electron-rich C^{IV}-B^{V} ("donor") bonds and the electron-deficient A^{III}-C^{IV} ("acceptor") bonds. We have reexamined the validity of a three-dimensional bulk thermodynamic model for $(GaAs)_{1-x}Ge_{2x}$ and $(GaP)_{1-x}Si_{2x}$ using an energy model that includes such electrostatic interactions and pairwise energies extracted from first-principles local-density total-energy calculations. The associated spin-1 Ising Hamiltonian is solved in the pair approximation of the cluster-variation method. A detailed thermodynamic description is given, including excess enthalpies, phase diagrams, and equilibrium solubilities. Electrostatic interactions stabilize the diamond phase and result in a major increase in the temperature range where both phases are stable. These changes, however, are insufficient to produce a second-order transition at the low (growth) temperatures and intermediate compositions where the transition is observed. While a previous controversy on the validity of thermodynamic models has focused on the question of whether the postulation of A^{III}-A^{III} and B^{V}-B^{V} bonds (needed to fit the observed critical compositions in such models) is consistent with independent evidence, we find that, with realistic values for the interaction parameters, the presence or absence of such bonds does not produce any significant change in the phase diagram below melting temperatures. We conclude that bulk thermodynamics is an inappropriate description of the problem. This opens the possibility that surface thermodynamics could be the physical mechanism that determines the final symmetry of the sample.

I. INTRODUCTION

Single-phase ternary $(A^{III}B^{V})_{1-x}C^{IV}_{2x}$ semiconductor alloys constitute a new class of metastable compounds with unusual structural and optical properties:[1,2] Unlike the constituents of the more common isovalent (III-V)/(III-V) and IV/IV alloys, $A^{III}B^{V}$ and C^{IV} are nearly mutually insoluble in the solid state,[3] even if they are size matched. This reflects the existence of local bonding arrangements that violate the octet rule,[4] e.g., the A^{III}-C^{IV} and B^{V}-C^{IV} bonds (whose total number of valence electrons deviates by $\Delta Z_v = \pm 1$ from the normal octet A^{III}-B^{V} and C^{IV}-C^{IV} bonds) and possibly A^{III}-A^{III} and B^{V}-B^{V} bonds ("wrong bonds" with total number of valence electrons deviating by $\Delta Z_v = \pm 2$ from the normal bonds). Despite their equilibrium segregating behavior, however, homogeneous nonisovalent alloys can be prepared by nonequilibrium growth methods. Indeed, $(GaAs)_{1-x}Si_{2x}$ alloys were synthesized already in 1974 by Noreika and Francombe.[5] Only in the past decade, however, have other $(A^{III}B^{V})_{1-x}C^{IV}_{2x}$ alloys, including $(GaSb)_{1-x}Ge_{2x}$,[6] $(GaAs)_{1-x}Ge_{2x}$,[7,8] and $(GaSb)_{1-x}Sn_{2x}$,[9] been successfully grown as homogeneous single phases. More recently, quaternary $(GaSb)_{1-x}Ge_{2x-2y}Sn_{2y}$ compounds have also been obtained.[10] Most of these alloys have been grown by sputter deposition, but some samples have been made by metal-organic chemical vapor deposition[8] (MOCVD) and molecular-beam-epitaxy[11] (MBE) techniques. In addition, many nonisovalent quaternary (III-V)/(II-VI) alloys have also been grown (see review in Ref. 12). Characterization studies of $(A_{III}B^{V})_{1-x}C^{IV}_{2x}$ systems have included Raman scattering,[13–15] crystallization thermodynamics,[16] x-ray diffraction,[17,18] extended x-ray-absorption fine structure[17] (EXAFS), transmission electron microscopy[11,15,19,20] (TEM), and ion channeling.[21]

These homogeneous $(A^{III}B^{V})_{1-x}C^{IV}_{2x}$ alloys exhibit a number of interesting properties: (i) While the optical band gaps of isovalent (III-V)/(III-V) or IV/IV alloys bow nearly parabolically and only slightly with composition[3] ($b \lesssim 1$ eV), the bowing in nonisovalent ternary $(A^{III}B^{V})_{1-x}C^{IV}_{2x}$ alloys[7,22,23] and quaternary (III-V)/(II-VI) alloys[12] can be more pronounced and significantly nonparabolic. (ii) The two interpenetrating fcc sublattices constituting the diamond lattice of C^{IV} can be occupied in $(A^{III}B^{V})_{1-x}C^{IV}_{2x}$ by either A^{III} or B^{V} atoms. If these sublattices are occupied *equally* by A^{III} and B^{V}, we have the pseudodiamond structure [Fig. 1(a)]; if, however, a sublattice is preferentially occupied by one of the two species, we have the pseudo-zinc-blende structure

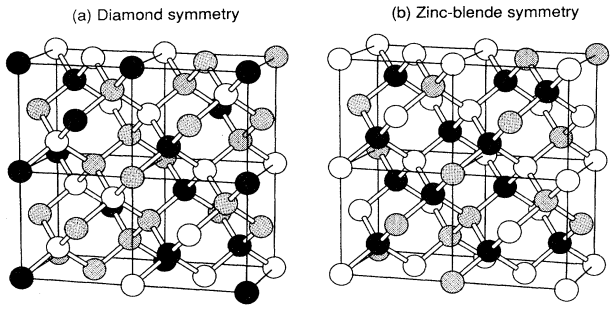

FIG. 1. Representation of structures with (a) the diamond and (b) the zinc-blende symmetry in $(A^{III}B^{V})_{1-x}C^{IV}_{2x}$ alloys. A solid circle indicates an A^{III} atom, an open circle a B^{V} atom, and a shaded circle a C^{IV} atom. For clarity, the structure in (b) represents the *maximum* possible zinc-blende ordering, with all A^{III} atoms on one sublattice and all B^{V} atoms on the other. Real zinc-blende samples may have *partial* zinc-blende ordering with both A^{III} and B^{V} atoms occupying (unequally) both sublattices.

[Fig. 1(b)]. While the latter structure is only partially ordered (in the sense that a given sublattice has a finite occupation by *both* species), we will refer to it as the "zinc-blende phase," or "ordered," since it manifests a [200] diffraction peak, which is forbidden in the simple diamond structure, but is observed in TEM (Ref. 11) and x-ray diffraction[17,18] of nonisovalent ternary systems. Indeed, a transition between the zinc-blende (ZB) structure of $A^{III}B^{V}$ and the simple diamond (D) structure of the C^{IV} component has been observed to occur at $x \approx 0.3$ in $(GaSb)_{1-x}Ge_{2x}$ (Refs. 17 and 18) grown by a multitarget rf sputtering technique at temperatures between 325 °C and 475 °C. A similar transition has been observed in $(GaAs)_{1-x}Ge_{2x}$ (Ref. 11) at $x \approx 0.3$ for samples grown by MBE at 430 °C and at $x \approx 0.4$ for samples grown by sputtering techniques.[18,24] [Ion-channeling studies,[21] however, suggest that a nonzero value of the ZB order parameter persists in $(GaSb)_{1-x}Ge_{2x}$ up to $x \approx 0.6$.]

The physical properties of nonisovalent systems have been the subject of numerous theoretical treatments. Many of these surround the properties of *ordered* systems: stability of superlattices,[25–29] band offset of superlattices,[26,27,29–33] growth models of Si/GaAs interfaces,[34,35] and impurity solution energies.[36] Others treated the bowing in disordered (III-V)/(II-VI) alloys.[12,37] Our main interest here lies in the understanding of the ZB↔D transition in $(A^{III}B^{V})_{1-x}C^{IV}_{2x}$ alloys.

The simplest theoretical approach to this problem is based on percolation theory.[38] In this approach the order-disorder transition is viewed as a pure geometrical and probabilistic phenomenon—namely, the appearance, beyond a critical concentration (called the "percolation threshold") of an infinite (or "percolating") connected cluster of the ordered component throughout the specimen. Since the percolation threshold for the diamond lattice is[39] $p_c = 0.428$, a simple model that prohibits $\Delta Z_v = \pm 2$ bonds (A^{III}-A^{III} and B^{V}-B^{V}) and considers percolation of the $A^{III}B^{V}$ component as the criterion for occurrence of the ZB phase[40] gives a critical concentration for the C^{IV} component of $x_c = 1 - p_c = 0.572$, below which the ZB phase occurs. This approach has been elaborated on by Holloway and Davis,[41,42] who added a new rule that forbids isolated A^{III} and B^{V} ions. This, however, leads to a still higher critical concentration ($x_c \approx 0.65$).

In addition to percolation approaches, there are two other points of view on the nature of the ZB↔D transition: growth models[43–45] and three-dimensional (3D) bulk thermodynamic models.[23,24,46,47] In "growth models"[43–45] one is attempting to directly produce a description of the atomic structure of the alloy without minimizing any explicit energy functional; one is instead emphasizing the significance of the *sequence* of growth as well as the *direction* of growth. This approach rests on defining a set of "growth rules" that dictate the preferences of incoming atoms to bond to specific substrate atoms; once bonded, atoms are assumed immobile. Since different substrate atoms are exposed in different substrate orientations, these rules naturally produce different geometries as the substrate orientation changes. These growth rules are not justifiable *a priori*, e.g., by way of an energy argument, but rather in terms of their success in producing an atomic structure that mimics *ex post facto* some of the properties of the experimentally observed structures. As a result, growth models produce structures that reflect the "deposition history" and are orientation dependent, but generally temperature independent. Subsequent to the modeling of the *structure*, one can apply to it an electronic Hamiltonian (e.g., tight binding) and solve for the electronic properties (e.g., through recursion solutions),[44] thus characterizing its optical response.

Three main attempt have been made at applying growth models to $(GaAs)_{1-x}Ge_{2x}$ alloys. Here, as in the percolation models, $\Delta Z_v = \pm 2$ bonds are usually forbidden. Kim and Stern[43] obtained a critical concentration of $x_c \approx 0.26$ in a simulation of [100] growth where stoichiometry is enforced by requiring identical behavior of the A^{III} and B^{V} species. The probabilities of attachment of Ge, Ga, and As were described by a single parameter (related to the final composition) and by disallowing Ga-Ga and As-As bonds. Davis and Holloway[44] proposed an alternative rule replacing the restriction of identical behavior of Ga and As: In their model, only Ga and Ge are initially attached, but an As atom necessarily bonds (on the following lattice plane) to a previously adsorbed Ga atom. This leads to $x_c \approx 0.3$ for [100] growth. When coupled to an electronic-structure calculation (tight-binding recursion method), this approach leads to a deep bowing of the direct band gap, as experimentally observed.[7,22,23] Both the Kim-Stern and the Davis-Holloway models stressed the dependence of x_c on the direction of growth. The Kim-Stern model has been extended by Preger *et al.*,[45] allowing for different sticking probabilities for the $\Delta Z_v = \pm 1$ A^{III}-C^{IV} and B^{V}-C^{IV} bonds than for the normal octet A^{III}-B^{V} and C^{IV}-C^{IV} bonds. The critical concentration was found to increase as the sticking probabilities of the $\Delta Z_v = \pm 1$ bonds de-

crease. The Kim-Stern and Preger *et al.* models differ in a basic way from the Davis-Holloway model: In the former, isolated A^{III} and B^{V} atoms are allowed, while in the latter, A^{III} and B^{V} atoms occur only as A^{III}-B^{V} molecules. Raman scattering data[15] have failed to detect a GaSb-like vibrational mode in $(GaSb)_{1-x}Ge_{2x}$ for concentrations $x > 0.75$; this tends to indicate that isolated substitutional Ga and Sb impurities in Ge are more probable in the $x \rightarrow 1$ alloy, in apparent disagreement with the Davis-Holloway model.

The second class of models applied to the ZB↔D transition are 3D "bulk" thermodynamic models.[23,24,46,47] There, one defines an interaction Hamiltonian that specifies the configurational dependence of the energy of the system and solves it in any of the available statistical-mechanics lattice models (e.g., mean field,[48] cluster-variation method,[49] or Monte Carlo simulations[50]). The basic premise of these models is that the atomic structure at a given (x,T) reflects a (local or global) minimum of a physically recognizable Hamiltonian. Again, once the structure is obtained, one can apply to it an electronic Hamiltonian that describes its electronic structure. In this approach, the *sequence* of growth does not enter (as atoms are assumed to be sufficiently mobile to attain any lattice configuration permitted by the Hamiltonian) and the orientation of growth does not alter the results (as a 3D symmetry is postulated). Hence, the results depend naturally on temperature but not on orientation. Note that these models are distinct from *surface* (2D) thermodynamic models that search for atomic configurations that minimize the free energy of a sample having a *free surface.* Such models are both temperature *and* orientation dependent as the surface-stable (or metastable) configuration is assumed to be frozen by the deposition of subsequent layers. Such an approach at $T=0$ was recently applied to pseudobinary alloys.[51]

Newman and collaborators[23,24] have applied a mean-field solution to the three-species (A^{III}, B^{V}, C^{IV}) lattice-statistics problem with only nearest-neighbor interactions (isomorphic to the spin-1 Blume-Emery-Griffiths model[52]). They have applied a virtual-crystal tight-binding calculation to the ensuing average structure, thus obtaining its electronic properties. If $\Delta Z_v = \pm 2$ bonds *are* allowed, an energy parameter of the model can be adjusted to give a ZB↔D transition at $x=0.3$. (Without such bonds,[47] however, the order-disorder transition occurs only at higher x values.) A discontinuity in the derivative of the direct gap with respect to x at this concentration has then been associated with the deep bowing observed[7,22,23] in $(GaAs)_{1-x}Ge_{2x}$. A better agreement with experiment is obtained when the simple mean-field lattice-statistics solution is replaced by the pair approximation of the cluster-variation method (CVM).[46,47] Note that in Newman *et al.*'s model, a critical concentration as low as 0.3 *requires* the presence of $\Delta Z_v = \pm 2$ bonds, but independent evidence for their existence remains controversial: It is possible to fit EXAFS (Ref. 17) results both without[17] and with[24,47] an assumption of the existence of $\Delta Z_v = \pm 2$ bonds. Raman scattering results,[13–15] on the other hand, fail to reveal the existence of an Sb-Sb mode in the $(GaSb)_{1-x}Ge_{2x}$ alloy. On the theoretical side, electronic-structure calculations (recursion-method[41,44] and coherent-potential-approximation[53]) agree that the presence of a significant number of As-As pairs in $(GaAs)_{1-x}Ge_{2x}$ would close the gap of the alloy over a wide composition range, contrary to experiment.

The relationships between the two basic approaches discussed above—the "growth models" and the "3D thermodynamic models"— were recently discussed.[54] It was pointed out that the growth models can be interpreted as two-dimensional three-state probabilistic cellular automata[55] and, as such, are mapped[56,57] onto a 3D Hamiltonian with *asymmetric* interactions: In the $(A^{III}B^{V})_{1-x}C^{IV}_{2x}$ alloy problem, the mapping assigns interactions to second neighbors that lie on a plane perpendicular to the growth direction and that are connected by an atom on the following plane. This breaks the symmetry of the 3D bulk solid. Such artificial Hamiltonians have not been previously applied to the $(A^{III}B^{V})_{1-x}C^{IV}_{2x}$ alloy problem. This asymmetry of the Hamiltonian constitutes the essential distinct feature of the growth models. It is reflected by a correlation-length critical exponent of the ZB↔D transition greater in the growth direction than perpendicular to it;[54] normal 3D bulk models naturally predict isotropic critical exponents.

Three main questions surround the application of 3D thermodynamic models to $(A^{III}B^{V})_{1-x}C^{IV}_{2x}$ alloys.

(a) Selection of values for interaction energies. In the Newman *et al.* models the Hamiltonian is parametrized in terms of *reduced energies* (in units of $k_B T$) so that specific values (or temperatures) remain unknown. However, a "cluster Bethe-lattice" tight-binding calculation[58] has obtained a value of 0.15 eV for the average $\Delta Z_v = \pm 1$ bond energy in $(GaAs)_{1-x}Ge_{2x}$. Using this value in the thermodynamic models leads to a transition temperature that is an order of magnitude too high compared with the experimental preparation temperatures. The non-self-consistent pseudopotential structural-expansion model of Ito[59] produces an average $\Delta Z_v = \pm 1$ bond energy of 0.16 eV for $(GaAs)_{1-x}Ge_{2x}$ and 0.17 eV for $(GaP)_{1-x}Si_{2x}$. No reliable self-consistent values exist, however, so accurate predictions of the transitions parameters have not been made.

(b) Physical content of the interaction Hamiltonian. In all previous applications,[23,24,46,47,58] it has been assumed that the interactions in the system consist of short-range concentration-independent energies between neutral atoms, so that the usual nearest-neighbor spin-1 Ising model[52] may be applied. However, unlike *isovalent* alloys, where such approaches are appropriate, *nonisovalent* alloys can exhibit significant charge-transfer effects with their attendant electrostatic interactions, neglected previously. This becomes clear when one realizes that an A^{III}-C^{IV} bond has a deficiency of $\frac{1}{4}$ of an electron (hence, behaving as an acceptor) and that a C^{IV}-B^{V} bond has an excess of $\frac{1}{4}$ of an electron (hence, behaving as a donor) and that transfer of a charge q from donor to acceptor states can reduce the electronic energy by the effective band-gap energy qE_g. Furthermore, the charge transfer produces intrabond Coulomb repulsion energy as well as an interbond long-range (Madelung) energy. Previous

models of the ZB↔D transition have neglected all these electrostatic terms. A recent work[29] on $(GaP)_n/(Si_2)_n$ and $(GaAs)_n/(Ge_2)_n$ superlattices demonstrated that the total energy (calculated in the local-density formalism[60] through a pseudopotential description[61]) can be accurately modeled by the above three electrostatic terms plus bond energies (the only type of term retained previously[23,24,46,47,58]), while neglecting such terms results in significant errors. This problem is well known in the theory of nonisovalent *impurities:* Creation of a neutral $(As_{Ga})^0$ antisite defect in GaAs plus an isolated neutral $(Ga_{As})^0$ antisite defect was calculated[62] to involve a formation energy as high as ≈ 6.3 eV/pair. This corresponds to the $q=0$ uncompensated case. However, transfer of two electrons from the $(As_{Ga})^0$ gap level to the $(Ga_{As})^0$ gap level [resulting in isolated $(As_{Ga})^{2+}$ and $(Ga_{As})^{2-}$] lowers this energy to ≈ 4.5 eV/pair. Upon permitting these two defects to interact, electrostatic effects further lower the energy, e.g., to 1.7 eV/pair when the two defects are nearest neighbors. The total energy lowering of 4.6 eV/pair reflects $q\neq 0$ effects that are analogous to these discussed here.

(c) Accuracy of the statistical solutions to a given Hamiltonian. No systematic comparison has been performed between simple mean-field[23,24] or pair-approximation cluster-variation method (CVM) results[46,47] and more accurate methods, like Monte Carlo simulations. It is expected, however, that pair-approximation CVM results, which are presumed to be exact in Bethe lattices,[63] are reasonably accurate in 3D noncompact structures (e.g., the diamond lattice) where relatively long paths (of at least six sites) are needed to achieve a closed loop. In fact, the spin-$\frac{1}{2}$ Ising model has a critical temperature in the pair approximation[49] just 6.7% above that obtained from an accurate series expansion.[64] In contrast,[65] simple (site-approximation) mean-field results are too high by as much as 48%.

In this paper we investigate a 3D thermodynamic model for $(A^{III}B^{V})_{1-x}C^{IV}_{2x}$ alloys that includes both pairwise (Ising-like) interactions and electrostatic interactions between bonds (effective three- and four-body interactions). The above-mentioned problems (a)–(c) surrounding the application of 3D thermodynamic models to nonisovalent alloys are treated as follows: (a) The interaction energies are extracted from first-principles self-consistent total-energy calculations[29] on prototype systems. (b) A realistic description of all three electrostatic effects is included. $\Delta Z_v=\pm 2$ bonds are disallowed and isolated ions are permitted to occur. (c) The lattice equilibrium thermodynamics is then obtained in the CVM pair approximation. These assumptions permit a realistic assessment of the true predictions of a 3D bulk theromodynamic approach. The resulting phase diagrams show that a 3D equilibrium thermodynamic interpretation for the observed ZB↔D transition does not explain experiment: While electrostatic interactions produce a major increase in the temperature ranges of stability of the two phases, coupled with a slight decrease in ZB↔D transition concentrations, these changes are significant only at temperatures that are $\gtrsim 1000$ K above the growth temperature where ordering occurs. This conclusion is independent of the presence or absence of $\Delta Z_v=\pm 2$ bonds in the model, if realistic values are used for these. This suggests that another type of thermodynamic description may be needed, e.g., a 2D thermodynamics that takes into account the growth process.[51]

The balance of this paper is organized as follows: Section II describes the charge-transfer energy model and identifies its different contributions to the excess energy of nonisovalent systems. The calculation of the corresponding energy parameters for GaP/Si and GaAs/Ge systems is presented in Sec. III, together with tests that support the accuracy of the model. Section IV describes how the energy model can be applied in a truncated form to alloys and defects. Section V introduces ideal maximum-entropy structures that permit the identification of the different contributions to the alloy excess energy in the two phases. Equilibrium alloys x-T phase diagrams are described in Sec. VI, which includes a discussion of low-temperature equilibrium solubilities and results from uncompensated and compensated alloys. Conclusions are presented in Sec. VII.

II. ENERGETICS OF NONISOVALENT SYSTEMS

We next consider the basic physical factors controlling nonisovalent interactions so that a realistic alloy Hamiltonian can be developed. While there is no experimental evidence for the presence of $\Delta Z_v=\pm 2$ bonds, energy arguments suggest that, if they occur in $(A^{III}B^{V})_{1-x}C^{IV}_{2x}$ alloys, they have a much smaller concentration than the $\Delta Z_v=\pm 1$ bonds. This can be estimated by contrasting calculated energies for $\Delta Z_v=\pm 2$ bonds (denoted W) and $\Delta Z_v=\pm 1$ bonds (denoted δ). Ito[59] estimated from a pseudopotential perturbation theory the change in internal energy ΔE(ZB/D) upon disordering a ZB binary compound into a diamondlike structure. This energy gives $\Delta E(\text{ZB/D})=W$ (per atom), where W is the excess energy of the average $\Delta Z_v=\pm 2$ bond, with respect to the normal octet A^{III}-B^{V} bond. He finds, for GaP, GaAs, and GaSb, that $W=0.68$, 0.65, and 0.57 eV, respectively, and that $\Delta Z_v=\pm 1$ bonds are as much as four times more stable. Baraff and Schlüter[62] find in their pseudopotential Green's-function calculations that the average energy of *uncompensated* As-As and Ga-Ga bonds is $6.3/8=0.79$ eV/bond (charge compensation reduces it substantially). The pseudopotential calculation of Lee *et al.*[27] for $(GaAs)_{1-x}Ge_{2x}$ superlattices gives $W=0.33$ eV and, for a $\Delta Z_v=\pm 1$ bond energy, $\delta=0.10$ eV. Davidovich *et al.*'s[58] tight-binding cluster–Bethe-lattice calculation for the $(GaAs)_{0.5}Ge_{1.0}$ alloy found $W=0.52$ eV and $\delta=0.15$ eV. In view of this evidence that $W\gg\delta>k_BT$ (where T is the temperature of preparation), we disallow structures with the $\Delta Z_v=\pm 2$ A^{III}-A^{III} and B^{V}-B^{V} bonds, permitting, however, the $\Delta Z_v=0$ A^{III}-B^{V} and C^{IV}-C^{IV} normal bonds and the $\Delta Z_v=\pm 1$ A^{III}-C^{IV} and C^{IV}-B^{V} bonds.

To model the energy of a nonisovalent system with normal and $\Delta Z_v=\pm 1$ bonds, we note that the latter bonds can be thought of as behaving as donors (C^{IV}-B^{V}) and acceptors (A^{III}-C^{IV}), each containing $\frac{1}{4}$ electron or

hole. Compensation can then occur through charge transfer from donor to acceptor bonds. This creates a distribution of positive and negative charges. The energy associated with this process can be conveniently modeled by considering $(A^{III}B^{V})_n/(C_2^{IV})_n$ superlattices (SL's). In superlattices, two types of $\Delta Z_v=\pm 1$ bond interfaces occur: In [110] SL's, both donor and acceptor bonds are present at the same ("neutral," or nonpolar) interface, while in [001] and [111] SL's, only one type of $\Delta Z_v=\pm 1$ bond is present at each (charged, or polar) interface. In unreconstructed [001] and [111] SL's, only partial compensation may take place if the period is long enough, since the band gap acts as an upper limit to the potential drop across charged interfaces. However, reconstruction can further lower the energy through swapping of atoms between interfaces, allowing thereby for a more effective compensation *within* each interface. Full compensation is expected in nonpolar [110] SL's and all other structures, including alloys, where long-range fields are absent.

According to the model of Dandrea, Froyen, and Zunger,[29] the excess energy of nonisovalent lattice-matched SL's can be approximated well by a combination of Ising-like nearest-neighbor interactions between neutral atoms and electrostatic terms due to charge transfer. Since the energies are measured with respect to the segregated end-point compounds, and since stoichiometry between the A^{III} and B^{V} elementary constituents is maintained, only the difference between the average energy of the two types of (neutral) $\Delta Z_v=\pm 1$ bonds and the average energy of the two types of normal bonds is a relevant parameter when electrostatic terms are not included. The total excess energy *before charge transfer* ($q=0$) is

$$E_{\text{pair}}(q=0)=(N_D+N_A)\delta \ , \tag{1}$$

where N_D and N_A are the total number of donor and acceptor bonds in the structure ($N_D=N_A$ for stoichiometric systems) and the average excess energy δ of the $\Delta Z_v=\pm 1$ bonds before charge transfer occurs is expressed in terms of bond energy differences as

$$\delta=\tfrac{1}{2}(\varepsilon_{\text{III-IV}}+\varepsilon_{\text{IV-V}}-\varepsilon_{\text{III-V}}-\varepsilon_{\text{IV-IV}}) \ . \tag{2}$$

After charge transfer, three additional terms appear.

(i) Transfer of a charge q from a donor to an acceptor state initially separated by a gap of $E_g(q=0)$ produces an energy gain (to first order in q) of $qE_g(q=0)$. A compensation gain,

$$E_{\text{comp}}=-\tfrac{1}{2}(N_D+N_A)E_g(0)q \ , \tag{3}$$

therefore arises.

(ii) The excess or deficit of compensated charges on the $\Delta Z_v=\pm 1$ bonds now produces an excess intrabond Coulomb energy, due to both electrostatic and exchange-correlation terms, given by

$$E_{\text{Coul}}=\tfrac{1}{4}(N_D+N_A)(U_D+U_A)q^2 \ , \tag{4}$$

where U_D and U_A are intrabond Coulomb repulsions in the donor and acceptor bonds.

(iii) Finally, an excess Madelung energy E_{Mad} results from the sum of screened long-range electrostatic interactions between compensating charges $\{q_i\}$ (usually $\frac{1}{4}$ and $-\frac{1}{4}$, in units of the electron charge) placed, in the model, at the midpoints $\{\mathbf{R}_i\}$ of the $\Delta Z_v=\pm 1$ bonds. (The small variations in bond length between donor and acceptor bonds[29] are ignored and the average bond length of the nearly lattice-matched $A^{III}B^{V}$ and C^{IV} constituents is used in the model.) These interactions are assumed to be screened, independently of distance, by the average static dielectric constant ϵ_0 of the two components, so that we have

$$E_{\text{Mad}}=\frac{e^2}{\epsilon_0}\sum_{i<j}\frac{q_iq_j}{|\mathbf{R}_i-\mathbf{R}_j|} \ . \tag{5}$$

The total excess energy is the sum of Eqs. (1) and (3)–(5):

$$\Delta H=E_{\text{pair}}(0)+E_{\text{comp}}+E_{\text{Coul}}+E_{\text{Mad}} \ . \tag{6}$$

Previous models[23,24,46,47,58] have retained only the $E_{\text{pair}}(0)$ term.

It is convenient for a thermodynamic treatment of the problem to regroup the contributions of Eqs. (1)–(5) as

$$\Delta H=E_{\text{pair}}(q)+E_{\text{Mad}} \ , \tag{7}$$

where

$$E_{\text{pair}}(q)=E_{\text{pair}}(q=0)+E_{\text{comp}}+E_{\text{Coul}} \ . \tag{8}$$

Here, $E_{\text{comp}}+E_{\text{Coul}}$ is the total-energy change that can be assigned to $\Delta Z_v=\pm 1$ bond energies due to charge transfer, including the (negative) compensation gain and the (positive) intrabond Coulomb energy. The total pairwise energy can also be written as

$$E_{\text{pair}}(q)=(N_D+N_A)J(q) \ , \tag{9}$$

where

$$J(q)=\delta+\Delta J(q) \ . \tag{10}$$

In this expression, the bond charge-transfer energy is

$$\Delta J(q)=-\tfrac{1}{2}E_g(0)q+\tfrac{1}{4}(U_D+U_A)q^2 \ . \tag{11}$$

In Sec. III we show how the energy parameters δ and (U_D+U_A) [and, therefore, $J(q=\frac{1}{4})$] are obtained from this model through first-principles superlattice pseudopotential total-energy calculations for the lattice-matched systems $(GaP)_n/(Si_2)_n$ and $(GaAs)_n/(Ge_2)_n$. The accuracy of this model in predicting calculated SL energies is then demonstrated.

III. CALCULATION OF ENERGY PARAMETERS AND TESTS OF THE MODEL

The excess energy and charge-transfer values were calculated[29] for 13 $(GaP)_n/(Si_2)_n$ SL's by the semirelativistic self-consistent pseudopotential method using a plane-wave basis with cutoff energy of 15 Ry. These were used to obtain a fit of the energy model of the previous section. The Madelung energy was calculated by the Ewald method,[66] with a dielectric constant[3] taken to be the average ($\epsilon_0=10.4$) of GaP and Si. The parameters δ and (U_D+U_A) were extracted from a least-squares fit to the

pseudopotential total energies for fixed values of $E_g(0)$. The degree of arbitrariness in the choice of $E_g(0)$ was of little consequence to the fit: Changes in $E_g(0)$ are offset by changes in (U_D+U_A) so that both $\Delta J(q)$ and δ are relatively insensitive to $E_g(0)$ over a reasonable range of values.

The resulting energy parameters for GaP/Si are $\delta=0.210$ eV and, for a full charge transfer, $J(q=\frac{1}{4})=0.126$ eV. The accuracy of the model is illustrated in Fig. 2, where energy values for some SL's calculated by the pseudopotential method ("P") are compared with those obtained by the model ("M"). The $q=0$ values give the prediction of the model for the uncompensated SL's. We find that all SL's have positive formation enthalpies ΔH, i.e., are unstable at equilibrium towards disproportionation, due to the presence of a large number of $\Delta Z_v=\pm 1$ bonds. Figure 2 illustrates the fact that charge transfer ($q=\frac{1}{4}$) makes the SL's less unstable. Since all SL's in Fig. 2(b) have the same number of donor and acceptor bonds, the model indicates that they have the same energy *if charge transfer is not allowed.* The model successfully explains the general trend in the deviations from the $q=0$ behavior in terms of the bond charge-transfer energy (including compensation gain and intrabond Coulomb terms) and the interbond Madelung interactions.

A similar fit was performed for the energy values of 11 $(GaAs)_n/(Ge_2)_n$ SL's for which nearly complete charge transfer occurs. The resulting energy parameters are $\delta=0.162$ eV and $J(q=\frac{1}{4})=0.109$ eV. Figure 3 compares the predictions of the model with the pseudopotential calculations, showing again good agreement.

Analysis of the directly calculated pseudopotential total energies in terms of our model permits assessment of the significance of various physical contributions. Compensation always acts to make the SL's less unstable. While the excess Madelung energy can be either positive or negative, the bond charge-transfer energy $\Delta J(q)$ is always negative, due to the prevalence of the $E_g(0)$ (compensation gain) term in Eq. (11) over Coulomb repulsions. Even when the excess Madelung energy is positive, it is never large enough to offset the gain in energy due to the bond charge-transfer term. The most extreme examples of SL stabilization by compensation occur for the [111] $n=1$ and [110] $n=2$ [Figs. 2(b) and 3(b)] cases, where large negative excess Madelung energies contribute to reduce the positive formation enthalpies to about half of their uncompensated $q=0$ values.

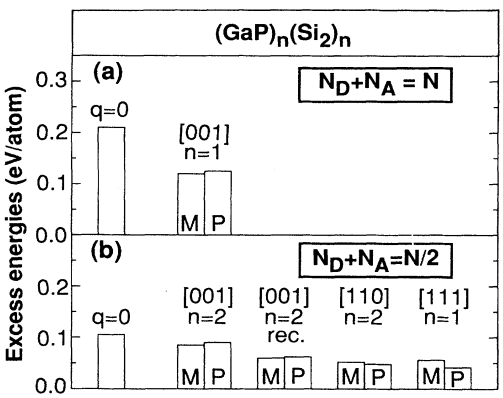

FIG. 2. Formation enthalpy (with respect to the separated constituents) of some $(GaP)_n/(Si_2)_n$ superlattices, according to the charge-transfer model (M) and to pseudopotential calculations (P) [Ref. 29]. The sublattices are classified in (a) and (b) according to their number of $\Delta Z_v=\pm 1$ bonds, N_D+N_A, and are denoted by their orientation and repeat period n. The bars for "$n=2$ rec" indicate the average energies of reconstructed structures obtained by swapping cation and anion atoms on different (001) planes, as described in Ref. 29.

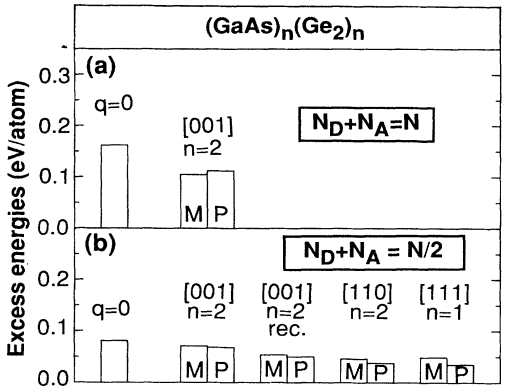

FIG. 3. Same as Fig. 2 for $(GaAs)_n/(Ge_2)_n$ superlattices.

All structures considered so far have equal atomic composition of the $A^{III}B^{V}$ and C^{IV} constituents. The question arises as to whether the present model can be applied directly to other structures of different compositions and to disordered or partially ordered alloys. In principle, the energy parameters of the model, especially $E_g(0)$ and δ, may depend on the composition. We test this by comparing the predictions of our energy model to a pseudopotential calculation[67] for periodic structures containing either Si_2 molecules in bulk GaP or diatomic GaP molecules in bulk Si, at a composition of $\frac{1}{8}$. This reveals that the energy model described above (parametrized at $x=\frac{1}{2}$) is a reasonable approximation even at those dilute limits: The pseudopotential calculations give $\Delta H=51$ meV/atom for Si_2 in GaP and 53 meV/atom for GaP in Si, in comparison with 43 meV/atom predicted by the model for both structures. These results indicate that compositional changes in $\Delta J(q)$ are partially offset by changes in δ.

Another issue concerning the validity of the energy model for alloys arises from the possibility of the presence of free carriers, due to thermal ionization of donor and acceptors. Such free carriers could possibly affect both the value of the band gap and the formation energy of the alloy. However, Hall measurements[11] for $(GaAs)_{1-x}Ge_{2x}$ suggest only weak n-type or p-type be-

havior, depending on composition and temperature of preparation, which supports the picture that nearly complete compensation occurs in the alloys.

In Sec. IV the present energy model is applied to alloys in an approximate treatment where the Madelung interactions are truncated to a few shells. This allows us to express our energy model in terms of a convenient statistical Hamiltonian.

IV. FINITE-RANGE MODEL FOR ALLOY AND DEFECT ENERGIES

Only the zinc-blende and diamond structures have been observed in $(A^{III}B^{V})_{1-x}C^{IV}_{2x}$ alloys.[11,17,18,24] Both structures lack a periodic arrangement of the compensated $\Delta Z_v = \pm 1$ bond charges. Since no C^{IV} sublattice ordering occurs, the probability for population of a given pair of nearest-neighbor sites by a negatively charged A^{III}-C^{IV} bond should be the same as that for a positively charged C^{IV}-B^{V} bond, where in both cases the first atom is taken to be located on the nominally cation sublattice. This is true even in the zinc-blende structure. It is hence expected that shells of bonds around a given bond are nearly neutral on average if the radius of the shell is large enough. It is therefore a reasonable approximation to truncate the terms in the alloy's Madelung energy [Eq. (5)] beyond a certain range, thus making the model amenable to an Ising-like description (see below). This is done by expressing the excess enthalpy of an $(A^{III}B^{V})_{1-x}C^{IV}_{2x}$ lattice-matched alloy [Eq. (7)] as

$$\Delta H = E_{\text{pair}}(q=\tfrac{1}{4}) + E_{\text{Mad}} \approx E_{\text{pair}}(q=\tfrac{1}{4}) + E_1 + E_2 + E_{3z} + E_{3h} \ , \quad (12)$$

where $E_{\text{pair}}(q=\frac{1}{4})$ is given by Eqs. (9)–(11) and E_1, E_2, E_{3z}, and E_{3h} are the contributions to the Madelung energy from first-neighbor bond pairs, second-neighbor bond pairs, third-neighbor bond pairs along a zigzag chain, and third-neighbor bond pairs in the same distorted hexagon, indicated in Fig. 4. We will see in Sec. V that this truncation is reasonable—e.g., for ideal maximum-entropy zinc-blende or diamond alloys, the contribution from E_{3h} is typically only 5% of E_1. The energy parameters E_n can be expressed as

$$E_n = N_n \sum_{i,j,k,l} p^{(n)}_{(ij)(kl)} C^{(n)}_{(ij)(kl)} \ , \quad (13)$$

where N_n is the total number of nth neighbor bond pairs on the lattice. The sum is taken over the possible occupations of nth neighbor bond pairs by (i,j) on one bond and (k,l) on the other. The probability $p^{(n)}_{(ij)(kl)}$ is the average fraction of $n$the neighbor bond pairs occupied by (i,j) and (k,l), and $C^{(n)}_{(ij)(kl)}$ is the corresponding interbond electrostatic interaction, given by

$$C^{(n)}_{(ij)(kl)} = \begin{cases} K^{(n)} & \text{for like } \Delta Z_v = \pm 1 \text{ bonds} \\ -K^{(n)} & \text{for unlike } \Delta Z_v = \pm 1 \text{ bonds} \\ 0 & \text{otherwise} \ . \end{cases} \quad (14)$$

The energy parameters $K^{(n)}$ can be calculated approximately from the average dielectric constant and from distances between bond centers; the resulting parameters for GaP/Si and GaAs/Ge SL's or alloys are given in Table I, together with the corresponding uncompensated (δ) and compensated [$J(q=\frac{1}{4})$] energies.

TABLE I. Energy parameters (in meV) for GaP/Si and GaAs/Ge systems: δ is the neutral $\Delta Z_v = \pm 1$ bond energy [Eq. (2)], $J(q=\frac{1}{4})$ is the compensated $\Delta Z_v = \pm 1$ bond energy [Eqs. (10 and (11)], and $K^{(n)}$ are the interbond Coulomb interactions [Eq. (14) and Fig. 4]. The last quoted digits are not supposed to be significant.

System	δ	$J(q=\frac{1}{4})$	$K^{(1)}$	$K^{(2)}$	$K^{(3)}$
GaP/Si	210	126	45	26	23
GaAs/Ge	162	109	35	20	17

To examine this truncated model, we give in Tables II and III the values of the different contributions to the formation enthalpy of unrelaxed $(GaP)_n/(Si_2)_n$ and $(GaAs)_n/(Ge_2)_n$ superlattices in three orientations. In addition, these tables display the results of the truncated model for idealized alloy systems whose structures are obtained by maximizing the configurational entropy of the zinc-blende and simple diamond phases subject to the constraint that $\Delta Z_v = \pm 2$ bonds are not allowed. The entropy has been obtained in the pair approximation of the cluster-variation method[49] (see Sec. V below). These tables compare the energy without electrostatic effects $\Delta H_M(q=0)$ [given by Eq. (1)] to that obtained by the full model ΔH_M without truncation, comparing the latter to direct pseudopotential calculations[29] ΔH_P, where available. The Madelung energy of Eq. (1) is broken into contributions of shells (Fig. 4), i.e., E_1, E_2, E_{3z}, and E_{3h}. Here, E_{rem} represents the remaining (infinitely numbered) terms in the excess Madelung energy of the alloy. Due to the long-range nature of electrostatic interactions and to the presence of ordered arrangements of charged bonds, in SL's E_{rem} is usually of the same order of magnitude of the $E_1, \ldots, E_{3h}$ terms. In alloys, however, a disordered distribution of charged bonds and the near charge neutrality of shells of a sufficiently large radius lead us to expect a relatively small E_{rem}. We see from Tables II and

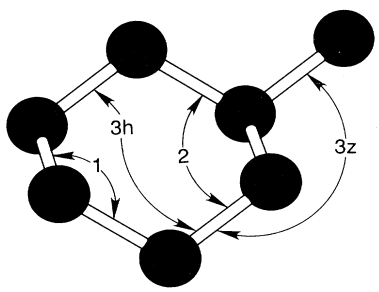

FIG. 4. Types of bond pairs, corresponding to the electrostatic interactions of Eq. (14).

TABLE II. Contributions to the formation enthalpies of unrelaxed GaP/Si superlattices and alloys. All energies are in meV/atom. $(N_D+N_A)/N$ gives the relative number of $\Delta Z_v=\pm 1$ bonds. The formation enthalpy in the model without charge transfer is $\Delta H_M(0)=E_{\text{pair}}(q=0)$ [Eq. (1)] and the pairwise energy with charge transfer is $E_{\text{pair}}(q)$ [Eqs. (9)–(11)]. The first few terms in the excess Madelung energy are shown next: Contributions E_n form nth neighbor bond pairs [Eqs. (13) and (14) and Fig. 4]. The remaining terms in the Madelung energy are denoted by E_{rem}, while the total excess Madelung energy is $E_{\text{Mad}}=E_1+E_2+E_{3z}+E_{3h}+E_{\text{rem}}$. The next two columns represent the total formation enthalpy from the model, $\Delta H_M=E_{\text{pair}}(q)+E_{\text{Mad}}$, compared to that from the pseudopotential calculation, ΔH_P [Ref. 29]. This comparison shows the model captures the important physical ingredients of the excess energy of nonisovalent systems. Superlattices of $(GaP)_n/(Si_2)_n$ are denoted by the repeat period n and orientation G. The line for "2 (rec)" displays average energies of reconstructed structures obtained by swapping cation and anion atoms on different (001) planes, as described in Ref. 29. The maximum entropy (Max-S) zinc-blende (ZB) and diamond (D) structures are described in Sec. V.

Structure		$\frac{N_D+N_A}{N}$	$\Delta H_M(0)$	$E_{\text{pair}}(q)$	E_1	E_2	E_{3z}	E_{3h}	E_{rem}	E_{Mad}	ΔH_M	ΔH_P
						Superlattices						
G	n											
[001]	1	1	210	126	45	−52	−23	−23	47	−6	120	125
	2	$\frac{1}{2}$	105	63	22	0	12	12	−24	22	85	90
	2(rec)	$\frac{1}{2}$	105	63	11	−26	0	0	12	−3	60	62
[110]	1	1	210	126	45	−52	−23	−23	47	−6	120	125
	2	$\frac{1}{2}$	105	63	0	−26	12	12	−8	−10	53	48
	3	$\frac{1}{3}$	70	42	0	−17	8	8	−5	−6	36	38
	4	$\frac{1}{4}$	52	32	0	−13	6	6	−4	−5	27	25
[111]	1	$\frac{1}{2}$	105	63	0	0	−34	34	−7	−7	56	42
	2	$\frac{1}{4}$	52	32	0	0	0	17	−12	5	37	30
	3	$\frac{1}{6}$	35	21	0	0	0	12	−3	9	30	25
						Alloys						
Max-S	ZB	1.097	230	138	56	−14	−6	2	a	38	176	
Max-S	D	1.172	246	148	46	−22	−10	4	a	18	166	

[a]Estimated to be small in alloys.

III that our model captures the variations in the directly calculated pseudopotential values and that neglect of electrostatic effects [compare $\Delta H_M(0)$ with ΔH_M] overestimates instability and reverses the order of the ZB and D alloy phases.

The truncated model can be used to predict the heats of solution of some simple substitutional nonisovalent defects in the $A^{\text{III}}B^{\text{V}}$ and C^{IV} constituents. Such results can be compared to those obtained from Harrison's universal-parameter tight-binding (UPTB) method[68] for isolated defects. Consider $(GaP)_{1-x}Si_{2x}$ as an example. We define the "sublattice heat of solution" $H_{\text{GaP}}(\text{Si,Si})$ as

TABLE III. Same as Table II for GaAs/Ge.

Structure		$\frac{N_D+N_A}{N}$	$\Delta H_M(0)$	$E_{\text{pair}}(q)$	E_1	E_2	E_{3z}	E_{3h}	E_{rem}	E_{Mad}	ΔH_M	ΔH_P
						Superlattices						
G	n											
[001]	1	1	162	109	35	−40	−17	−17	35	−4	105	112
	2	$\frac{1}{2}$	81	54	18	0	8	8	−18	16	70	68
	2(rec)	$\frac{1}{2}$	81	54	9	−20	0	0	9	−2	52	50
[110]	1	1	162	109	35	−40	−17	−17	35	−4	105	112
	2	$\frac{1}{2}$	81	54	0	−20	8	8	−5	−9	45	38
	3	$\frac{1}{3}$	54	36	0	−13	6	6	−4	−5	31	35
	4	$\frac{1}{4}$	40	27	0	−10	4	4	−2	−4	23	22
[111]	1	$\frac{1}{2}$	81	54	0	0	−26	26	−5	−5	49	35
						Alloys						
Max-S	ZB	1.097	178	120	44	−11	−4	2	a	31	151	
Max-S	D	1.172	189	128	36	−17	−7	3	a	15	143	

[a]Estimated to be small in alloys.

the energy required to transfer a pair of unbound Si atoms from the bulk of a Si crystal replacing a pair of Ga and P atoms in GaP, so that the two Si atoms remain separated in two different sublattices.[69] This creates four Si—Ga and four compensating Si—P bonds in tetrahedral geometries. Each defect, therefore, carries an additional electrostatic energy due to repulsions of six pairs of charged bonds. An equal value is predicted by the model for the heat of solution $H_{Si}(Ga,P)$ of an unbound pair of a Ga and a P atom in Si (now no sublattice considerations are necessary). We hence define the average[70] of the two heats of solution as

$$\Delta\mathcal{E}_1(q)=[H_{GaP}(Si,Si)+H_{Si}(Ga,P)]/2$$
$$=8J(q=\tfrac{1}{4})+12K^{(1)} . \quad (15)$$

For the $q=0$ uncompensated case, the model predicts simply

$$\Delta\mathcal{E}_1(q=0)=8\delta . \quad (16)$$

The results for the average sublattice heats of solution of unbound pairs are given in Table IV, where they are compared with those obtained (for GaAs/Ge) from the cluster–Bethe-lattice tight-binding calculation of Davidovich *et al.*[58,71] (DKOR) and with those from the Harrison-Kraut[36,72] (HK) UPTB calculation.

We can also predict the heats of solution of *bound* pairs of atoms. The heat of solution $H_{GaP}(Si_2)$ is defined as the energy required to transfer a Si_2 molecule from the bulk of a Si crystal into a GaP crystal,[69] where one Si atom occupies a cation site and the other occupies a nearest-neighbor anion site. Such a process involves the creation of three Si—Ga and three compensating Si—P bonds and corresponding interbond electrostatic interactions. The model predicts an identical result for the heat of solution $H_{Si}(GaP)$ of a bound GaP molecule in Si, so that their average is given by

$$\Delta\mathcal{E}_2(q)=[H_{GaP}(Si_2)+H_{Si}(GaP)]/2$$
$$=6J(q=\tfrac{1}{4})+6K^{(1)}-6K^{(2)}-3K^{(3)} . \quad (17)$$

For the uncompensated $q=0$ case, we have

$$\Delta\mathcal{E}_2(q=0)=6\delta . \quad (18)$$

These results for the heats of solution of bound pairs are given in Table IV. The results for GaAs/Ge can be compared with that from the DKOR calculation.

The sublattice heats of solution of unbound pairs $\Delta\mathcal{E}_1$ is in reasonable agreement with the UPTB theory, especially for GaP/Si. Note that charge transfer reduces significantly $\Delta\mathcal{E}_2$, but has a small effect on the energy $\Delta\mathcal{E}_1$ of unbound pairs. We also emphasize that in the present model the split in the energies of the bound ($\Delta\mathcal{E}_2$) and unbound ($\Delta\mathcal{E}_1$) pairs is enhanced by the interbond electrostatic interactions, as is evident from the comparison between our results for the compensated ($q=\frac{1}{4}$) and uncompensated ($q=0$) cases, or between our compensated results and those from the DKOR theory, where no charge-transfer effects have been introduced.

In the following sections this model is applied to ideal maximum-entropy alloys with zinc-blende and diamond atomic arrangements. This permits the identification of the individual contributions to the energy of the two phases, and the calculation of the equilibrium phase diagrams (see Sec. VI) for such systems.

V. MAXIMUM-ENTROPY STRUCTURES

In order to obtain a general idea of the individual contributions to the energy of the zinc-blende (ZB) and diamond (D) phases in an $(A^{III}B^{V})_{1-x}C^{IV}_{2x}$ alloy (rather than SL's or impurity systems), it is instructive to consider first some ideal alloys that are closest to a random ($T\rightarrow\infty$) arrangement of atoms with either the ZB or the D symmetry, subject to the constraint of no A^{III}-A^{III} or B^{V}-B^{V} bonds. The stability of the two phases will then be related to a three-species correlated percolation problem.[73] In Sec. VI we consider finite-temperature effects; extending these results to $T\rightarrow\infty$ recovers the "maximum-entropy" structures considered in this section.

To find the maximum-entropy structures, we use Kikuchi's cluster-variation method[49] (CVM) with a pair as a basic cluster. Here, correlations within a nearest-neighbor pair of sites are adequately taken into consideration. In the present problem, pair correlations are driven by the prohibition of $\Delta Z_v=\pm 2$ bonds and are expected to decay rapidly with distance. Denoting the two

TABLE IV. Average sublattice heats of solution (in eV per pair of impurities) of A^{III} and B^{V} impurities in a C^{IV} host crystal and C^{IV} impurities in an $A^{III}B^{V}$ host crystal, according to the present model [Eqs. (15)–(18)] and to previous tight-binding calculations. The energy of an unbound pair, $\Delta\mathcal{E}_1$, is given by Eq. (15) for $q=\frac{1}{4}$ and Eq. (16) for $q=0$, while that of a bound pair, $\Delta\mathcal{E}_2$, is given by Eq. (17) for $q=\frac{1}{4}$ and Eq. (18) for $q=0$.

			Present Model			
$A^{III}B^{V}$	C^{IV}	Pair	$q=\frac{1}{4}$	$q=0$	HK[a]	DKOR[b]
GaP	Si	Unbound ($\Delta\mathcal{E}_1$)	1.55	1.68	1.44	
		Bound ($\Delta\mathcal{E}_2$)	0.80	1.26		
GaAs	Ge	Unbound ($\Delta\mathcal{E}_1$)	1.29	1.30	0.90	1.20
		Bound ($\Delta\mathcal{E}_2$)	0.69	0.97		0.90

[a]Harrison and Kraut, Ref. 36, using the "universal parameter tight-binding" method.
[b]Davidovich *et al.*, Ref. 58, using the tight-binding cluster–Bethe-lattice method.

fcc sublattices of the diamond lattice by α and β, we call y_{ij} the pair probability for finding an atom i on sublattice α and a neighboring atom j on sublattice β. The corresponding site probabilities will be denoted by x_i^α and x_j^β. The total configurational entropy of the lattice per site in units of k_B is then approximated by[49]

$$\frac{S}{Nk_B}=-2\sum_{i,j}\mathcal{L}(y_{ij})+\tfrac{3}{2}\sum_i\mathcal{L}(x_i^\alpha)+\tfrac{3}{2}\sum_j\mathcal{L}(x_j^\beta)\ , \qquad (19)$$

where $\mathcal{L}(u)\equiv u\ln u$ and the indices i and j identify the three possible species ($i=-1,0,1$ for elements $A^{\rm III},C^{\rm IV},B^{\rm V}$, respectively) on each site. This entropy is then maximized (e.g., by Kikuchi's natural iteration method[74]) with the constraint that no $\Delta Z_v=\pm 2$ bonds occur and subject to the sum rules

$$x_i^\alpha=\sum_j y_{ij}\ ,\quad x_j^\beta=\sum_i y_{ij}\ ,\quad 1=\sum_i x_i^\alpha=\sum_j x_j^\beta\ , \qquad (20)$$

with $x_0^\alpha+x_0^\beta=2x$. The ZB phase is characterized by a nonzero order parameter

$$z_1=x_1^\alpha-x_{-1}^\alpha=x_{-1}^\beta-x_1^\beta$$

(z_1 is zero in the D phase). The result of the entropy maximization indicates a second-order transition between the ZB and the D phases at $x=x_p\approx 0.57$. Below this critical concentration, the ZB phase has a larger entropy than the D phase and is therefore more stable in the infinite-temperature limit (neglecting, however, melting of the crystal). This apparent contradiction of a larger configurational entropy for the more ordered ZB phase simply indicates that, for $x<x_p$, there are (many) more lattice configurations with an infinite (percolating) $A^{\rm III}B^{\rm V}$ cluster (leading to a nonzero sublattice order parameter) than configurations with only finite clusters.

The identification of the maximum-entropy structures now enables the calculation of the various contributions to their energies using the model of Sec. IV. It can be noticed from Tables II and III that the relative number of $\Delta Z_v=\pm 1$ bonds $[(N_D+N_A)/N]$ is larger in the D phase than in the ZB phase, leading to a larger excess enthalpy for the D phase *if charge transfer is disallowed.* The Madelung contribution to the excess enthalpy of the alloy in the two phases can be estimated with the use of "superposition approximations"[75–77] for the occupation probabilities of clusters larger than the pair. For instance, the occupation of a three-site α-β-α figure made of two bonds with a common site β is given by

$$q_{ijk}^{\alpha\beta\alpha}=\frac{y_{ij}y_{kj}}{x_j^\beta}\ . \qquad (21)$$

The total-energy expression in the superposition approximation is presented in Sec. VI and Appendix A.

In the results displayed in Fig. 5 for $(GaP)_{1-x}Si_{2x}$, we have divided the excess enthalpy of the alloy into the pairwise energy $E_{\rm pair}$ [Eq. (8)] and the Madelung (interbond electrostatic) energy $E_{\rm Mad}$ [Eq. (12)]. (The continuations of the D curves for $x<0.57$ represent an unstable branch.) Although both contributions are positive, the alloy has a smaller excess enthalpy with charge transfer than without it. Figure 6 illustrates the typical energy distribution in the two phases for $x<x_p$, where the ZB phase is thermodynamically stable. We note the following.

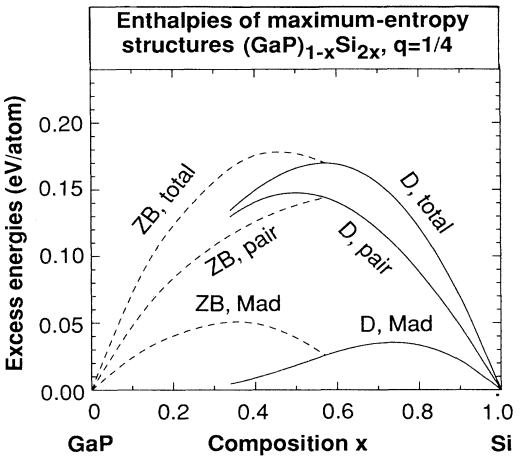

FIG. 5. Excess enthalpies (with respect to the separated constituents) of the maximum-entropy $(GaP)_{1-x}Si_{2x}$ alloys in the zinc-blende (ZB) and diamond (D) phases, with no Ga—Ga or P—P bonds, as obtained in the pair approximation of the cluster-variation method. The contributions from (Ga—Si and Si—P bonds) pairwise energies [Eq. (8)] and interbond Madelung terms ($E_{\rm Mad}$) [Eq. (12)] are shown. The zinc-blende phase is indicated by dashed curves and the diamond phase by solid curves.

(i) The Madelung energy $E_{\rm Mad}$ is higher in the ZB phase than in the D phase. The reason for this can be understood by considering the three-site figure of Eq. (21): In the ZB phase, more Ga-Si-Ga and P-Si-P clusters

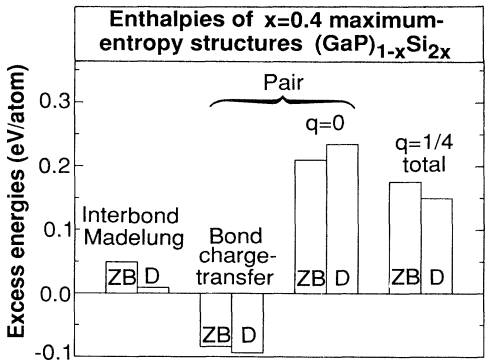

FIG. 6. Excess enthalpies of the $x=0.4$ maximum-entropy $(GaP)_{1-x}Si_{2x}$ alloys. The "pair" contribution has been separated into the uncompensated $q=0$ term [Eq. (1)] and the "bond charge-transfer" term $E_{\rm comp}+E_{\rm Coul}$ [Eqs. (3) and (4)]. The "interbond Madelung" term is given by Eq. (12) and the "$q=\frac{1}{4}$ total" by Eq. (7).

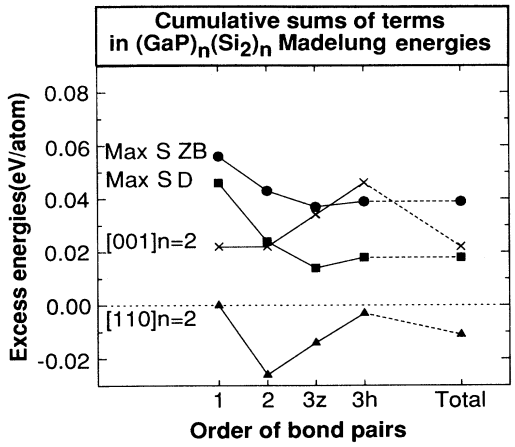

FIG. 7. Convergence of the excess Madelung energies of maximum-entropy (Max-S) $x=0.5$ $(GaP)_{1-x}Si_{2x}$ alloys in the zinc-blende (ZB) and diamond (D) phases and of two $n=2$ $(GaP)_n/(Si_2)_n$ superlattices. The order of bond pairs correspond to the electrostatic interactions of Fig. 4.

(where either Ga *or* P is located on one sublattice) and less Ga-Si-P (where Ga *and* P are located on the same sublattice) are found; the electrostatic repulsion between $\Delta Z_v=\pm 1$ bonds of the same kind then increases the energy of the ZB phase.

(ii) The bond charge-transfer energy $E_{\rm comp}+E_{\rm Coul}$ [Eqs. (3) and (4) and Fig. 6] is higher (less negative) in the ZB phase. This is due to a larger number of Ga and P atoms on the "correct" sublattices, leading to a larger number of Ga—P normal bonds and, therefore, a smaller number of Ga—Si and Si—P ($\Delta Z_v=\pm 1$) bonds. Consequently, the compensation energy (which stabilizes both phases) is less negative in the ZB phase.

(iii) The "chemical" part of the pairwise energy, $E_{\rm pair}(q=0)$, is smaller in the ZB phase for the same $\Delta Z_v=\pm 1$ bond counting argument given in item (ii).

As a combined result of effects (i), (ii), and (iii), we find (a) a smaller excess enthalpy for both phases in comparison with the no-charge-transfer results and (b) a smaller excess enthalpy for the D phase than for the ZB phase, in contrast with the no-charge-transfer result. Effect (a) implies that both phases are stabilized with respect to models with no charge transfer, while effect (b) indicates that the region of stability of the D phase in the phase diagram is expected to increase at finite temperatures.

The convergence of the excess Madelung energies of the alloys as successive shells are included in the sum is illustrated in Fig. 7 for $x=0.5$ in maximum-entropy $(GaP)_{1-x}Si_{2x}$ alloys and in two corresponding SL's. It is verified that, while the SL's can show drastic variations of the cumulative Madelung sum as more terms are introduced, a smoother and rapidly converging behavior is found in the *alloys*. This justifies our truncation of Eq. (12).

VI. EQUILIBRIUM PHASE DIAGRAMS

A. Hamiltonian and its solution

We discuss next the equilibrium finite-temperature thermodynamics resulting from our truncated charge-transfer model using the pair approximation of the cluster-variation method (CVM). We will comment on both equilibrium results and on possible metastable states.

The bulk equilibrium thermodynamics of homogeneous $(A^{\rm III}B^{\rm V})_{1-x}C^{\rm IV}_{2x}$ solid alloys will be described through the excess free energy

$$\Delta F=\Delta H-TS\ , \tag{22}$$

where the excess enthalpy ΔH includes the pairwise and interbond electrostatic terms of Eq. (7) and the configurational entropy S is given in the CVM pair approximation of Eq. (19). In terms of the pair probabilities $\{y_{ij}\}$, the excess enthalpy is written as

$$\Delta H=2N\sum_{i,j}y_{ij}\,b_{ij}+\sum_n N_n\sum_{i,j,k,l}p^{(n)}_{(ij)(kl)}\,C^{(n)}_{(ij)(kl)}\ , \tag{23}$$

where

$$b_{ij}=\begin{cases}J(q) & \text{for } \Delta Z_v=\pm 1 \text{ bonds}\\ 0 & \text{otherwise}\ ,\end{cases} \tag{24}$$

and the factors in the second term are defined in the text immediately before Eq. (14). Using the superposition approximation discussed in Appendix A, the three-site $\{p^{(1)}_{(ij)(jk)}\}$ and four-site $\{p^{(n)}_{(ij)(kl)}\}$ $(n>1)$ probabilities are expressed in terms of the pair probabilities $\{y_{ij}\}$ by Eqs. (A1)–(A4) of Appendix A. The total number of each type of pairs of bonds is given by

$$N_1=6N\ ,\quad N_2=12N\ ,\quad N_{3z}=N_{3h}=6N\ . \tag{25}$$

At a given concentration x and temperature T, the CVM free energy will be minimized with respect to the basic cluster (pair) probabilities $\{y_{ij}\}$ to give the equilibrium values of these probabilities (and therefore of any desired thermodynamic function). Since we include interactions of longer range than the size of the basic cluster, the superposition approximation produces terms in the formation enthalpy that are nonlinear with respect to the pair probabilities. Therefore, the straightforward "natural iteration" method[74] is not guaranteed to converge. Instead, we minimize the free energy with respect to the complete set of independent correlation functions defined below.

A three-species problem in the pair approximation has at most $3^2-1=8$ minimization variables. In the present problem, this number is reduced to 3 by requiring that no $\Delta Z_v=\pm 2$ bonds are present and by using additional symmetries resulting from the presence of the same (fixed) number of $A^{\rm III}$ and $B^{\rm V}$ atoms, as shown by the following argument. According to the "spin-1 cluster algebra,"[78] we can define a set of correlation functions $\{\xi_n\}$ (which are independent variables if no constraint exists among the pair probabilities $\{y_{ij}\}$ other then the normalization $\sum_{ij}y_{ij}=1$), given by

$$\xi_1=\langle S_i\rangle\ ,\quad \xi_2=\langle S_j\rangle\ ,$$
$$\xi_3=\langle S_i^2\rangle\ ,\quad \xi_4=\langle S_j^2\rangle\ ,$$
$$\xi_5=\langle S_iS_j\rangle\ ,\quad \xi_6=\langle S_i^2S_j^2\rangle\ ,$$
$$\xi_7=\langle S_i^2S_j\rangle\ ,\quad \xi_8=\langle S_iS_j^2\rangle\ . \tag{26}$$

Here, i and j represent nearest-neighbor sites on sublattices α and β, respectively; the spin variable S_i can assume the values -1, 0, or 1, according to which atomic species ($A^{\rm III}$, $C^{\rm IV}$, or $B^{\rm V}$, respectively) is located on site i; and $\langle\cdots\rangle$ indicates a thermodynamic average. The "spin-1 cluster algebra"[78] can be used to express the site and pair probabilities as linear combinations of the correlation functions.

The restriction that $\Delta Z_v=\pm 2$ bonds [$(++)$ and $(--)$ occupations of the basic cluster] are not present implies

$$\xi_5=-\xi_6\ ,\quad \xi_7=-\xi_8\ . \tag{27}$$

For alloys with the same number of $A^{\rm III}$ and $B^{\rm V}$ atoms, we have

$$\xi_1=x_+^\alpha-x_-^\alpha=-\xi_2=x_-^\beta-x_+^\beta\ . \tag{28}$$

Finally, we assume that no sublattice ordering of the $C^{\rm IV}$ atoms exists. Such an ordering is energetically unfavorable since it would create an excessive amount of $\Delta Z_v=\pm 1$ bonds. (A more rigorous argument for the absence of $C^{\rm IV}$ sublattice ordering is presented later in Appendix B.) This implies

$$\xi_3=\xi_4=1-x\ . \tag{29}$$

Therefore, for a fixed composition x, the only independent correlation functions are

$$z_1=\langle S_i\rangle=x_+^\alpha-x_-^\alpha=x_-^\beta-x_+^\beta\ ,$$
$$z_2=\langle S_iS_j^2\rangle=y_{+-}-y_{-+}\ , \tag{30}$$
$$z_3=\langle S_i^2S_j^2\rangle=y_{+-}+y_{-+}\ .$$

The correlation functions z_1 and z_2 are long-range order parameters, which vanish in the diamond phase, while z_3 is a short-range order parameter. The deviation of z_3 from its mean-field value, $x_+^\alpha x_-^\beta+x_-^\alpha x_+^\beta$, is an important improvement of the pair approximation (over the site mean-field theory) that allows for the exclusion of $\Delta Z_v=\pm 2$ bonds in the model. The site and pair probabilities are expressed in terms of the correlation functions.[78] The excess free energy is therefore expressed as a functional $\Delta F(\{z_i\};x,T)$, which is then minimized with respect to the $\{z_i\}$. The CVM minimization scheme usually does not converge at low temperatures. In our case, the limits of phase separation below approximately 1400 K in $(GaP)_{1-x}Si_{2x}$ and 1200 K in $(GaAs)_{1-x}Ge_{2x}$ (for the compensated alloys) have been extrapolated from the higher-temperature results. The resulting phase diagrams are displayed in Fig. 8 [for $(GaP)_{1-x}Si_{2x}$] and Fig. 9 [for $(GaAs)_{1-x}Ge_{2x}$].

B. Low-temperature equilibrium solubilities

We discuss now the low-temperature behavior of the solutions. The following model assumes that only isolated impurities occur in the dilute ($x\to 0$ and $x\to 1$) limits of $(A^{\rm III}B^{\rm V})_{1-x}C_{2x}^{\rm IV}$ alloys. An intermediate regime where clusters of impurities are formed, between the regimes of (i) isolated impurities and (ii) phase separation, is neglected. The results are therefore expected to give esti-

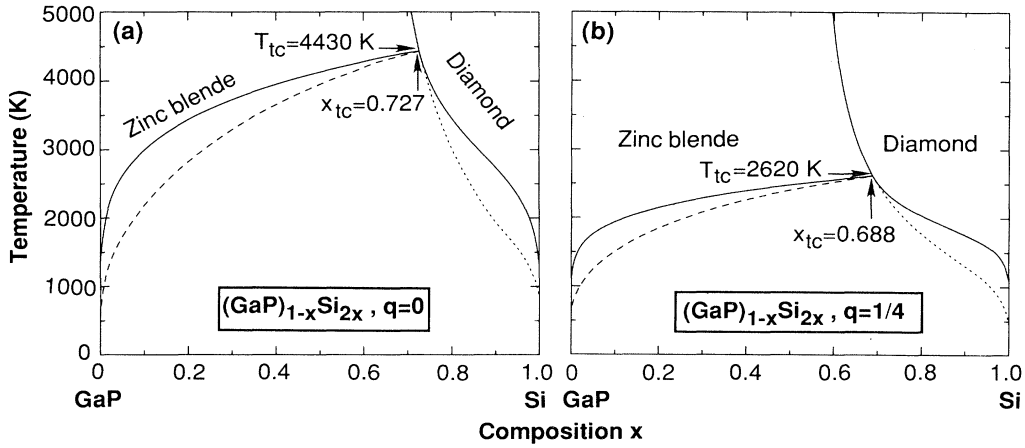

FIG. 8. Equilibrium phase diagram for the $(GaP)_{1-x}Si_{2x}$ alloy (a) without and (b) with charge transfer. The region below the tricritical point (x_{tc},T_{tc}) and between the two solid lines corresponds to phase separation into GaP-rich zinc-blende and Si-rich diamond phases. The dashed line is the spinodal of the zinc-blende phase. The dotted line is the unstable continuation of the second-order transition line.

mates for order of magnitudes of solubilities.

A C^{IV} impurity atom in solid $A^{III}B^{V}$ has an excess energy $\Delta\mathcal{E}_1/2$, where $\Delta\mathcal{E}_1$ is given by Eq. (16) if no charge-transfer effects are included or Eq. (15) with charge-transfer effects. In the very dilute limit no correlation occurs between different impurities, and a mean-field expression for the entropy is appropriate. The free energy in the $x \to 0$ limit is then given by

$$F_0(x)=Nx\frac{\Delta\mathcal{E}_1}{2}-k_BT\ln\frac{N!}{(Nx)![N(1-x)]!}$$
$$=N\frac{\Delta\mathcal{E}_1}{2}\left[x+\frac{2k_BT}{\Delta\mathcal{E}_1}[x\ln x+(1-x)\ln(1-x)]\right]. \quad (31)$$

A similar expression is found in the $x \to 1$ limit, but now it is necessary to consider the possible occupations of a given site by the two types of impurities (A^{III} and B^{V}) in C^{IV}. In this limit we consider the case where the concentration is the same $[(1-x)/2]$ for the two types of impurities. We have then

$$F_1(x)=N(1-x)\frac{\Delta\mathcal{E}_1}{2}-k_BT\ln\frac{N!}{(Nx)!2[N(1-x)/2]!}$$
$$=N\frac{\Delta\mathcal{E}_1}{2}\left[1-x+\frac{2k_BT}{\Delta\mathcal{E}_1}\left[x\ln x+(1-x)\ln\frac{1-x}{2}\right]\right]. \quad (32)$$

The phase separation region is determined by the common-tangent construction.[74] It is found that the common tangent to $F_0(x)$ and $F_1(x)$ passes *near* the *minima* of $F_0(x)$ and $F_1(x)$, which occur, respectively, at

$$x_0\simeq\exp\frac{-\Delta\mathcal{E}_1}{2k_BT} \quad (33)$$

and

$$1-x_1\simeq 2x_0\ . \quad (34)$$

In these equations, x_0 represents the equilibrium solubility of C^{IV} atoms in solid $A^{III}B^{V}$, and x_1 the equilibrium solubility of an equal number of A^{III} and B^{V} atoms in solid C^{IV}. The model predicts very small *equilibrium* solubilities of the nonisovalent substitutions at solid-state temperatures, as observed experimentally.[79] For instance, for compensated Ge in GaAs, we get from Eq. (33) and Table I (with $q=\frac{1}{4}$), $x_0\approx 6\times10^{-4}$ at 1000 K and 4×10^{-6} at 600 K. Note, however, that these values are substantially larger than those obtained with no charge transfer (with $\Delta\mathcal{E}_1$ given by the $q=0$ value in Table IV). In this case, we get $x_0\approx 3\times10^{-7}$ at 1000 K and 1×10^{-11} at 600 K. This increase of the solubility with compensation implies that pairs of impurities of complementary valence, e.g., Ga and As in Si or Zn and Se in GaAs, where the total $\Delta Z_v=0$, are more soluble than either impurity separately.

C. Results for the $q=0$ uncompensated case

We analyze next the uncompensated $q=0$ phase diagrams, presented in Figs. 8(a) and 9(a). Note that the two diagrams are equivalent to each other, except for a scaling of the temperature axis with k_BT/δ, and correspond to a special case of the Blume-Emery-Griffiths spin-1 Ising model. The isomorphism between the two models is presented in Appendix B.[47,80–83] Phase diagrams for this uncompensated case have been previously presented by Gu *et al.*[47] with a temperature axis in units of the A^{III}-B^{V} bond energy.[84] The following notable features are found in these phase diagrams.

(i) In the infinite-temperature limit, we recover the maximum-entropy case discussed in Sec. V with a second-order transition between the ZB and the D phases at $x\approx 0.57$. In contrast, phase diagrams for models that include $\Delta Z_v=\pm2$ bonds[23,46,47] show the ZB↔D second-

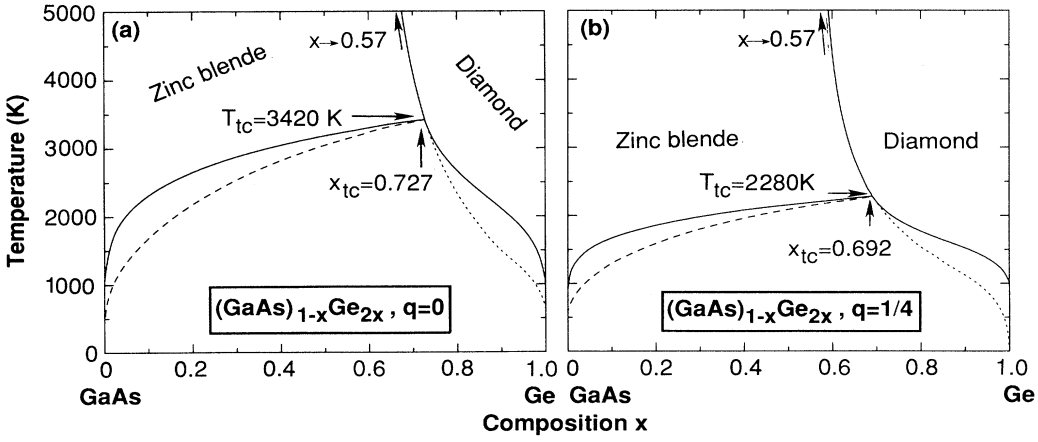

FIG. 9. Same as Fig. 8 for $(GaAs)_{1-x}Ge_{2x}$.

order transition line terminating at $x=0$ at a finite critical temperature T_c, so that only the D phase is stable for $T>T_c$. This feature enabled a low ($x_c=0.3$ or 0.4) order-disorder concentration to be *fitted* in previous approaches by adjusting ratios of temperature to interaction energies. While we have excluded $\Delta Z_v=\pm 2$ bonds, we note that if their energy were three to four times δ (as suggested in Refs. 27, 58, and 59), their inclusion in our model would lead to significant deviations in the phase diagrams only for $T\gtrsim 2000$ K.

(ii) As the temperature is lowered, x_c increases gradually, until a *tricritical point* is reached, at $T=T_{tc}=1.82\delta/k_B$, $x=x_{tc}=0.727$, below which the transition becomes first order. The presence of a tricritical point is a well-known characteristic of the Blume-Emery-Griffiths model.[52]

(iii) Below the tricritical point, the first-order transition is reflected in an (x,T) diagram by a phase-separation region, whose concentration range increases rapidly as the temperature drops until it occupies the whole $0<x<1$ interval at $T=0$. Two curves inside this phase-coexistence region are relevant for the discussion of possible metastable states. The meaning of these curves is best illustrated with the aid of a constant-temperature F versus x curve, as presented in Fig. 10. [Although the example of Fig. 10 was taken from the calculation for a compensated $(GaAs)_{1-x}Ge_{2x}$ alloy, the behavior is similar for the uncompensated cases.] (a) The dashed line in Figs. 8 and 9 from $(x,T)=(0,0)$ to (x_{tc},T_{tc}) is the ZB-phase spinodal,[85] where $\partial^2 F/\partial x^2=0$, and corresponds to point S in Fig. 10. To the right of point S in Fig. 10, the single-phase ZB solution, although still a minimum of the CVM free energy, does not satisfy the condition $\partial\mu/\partial x>0$ of thermodynamic stability,[65] where $\mu=N^{-1}\partial F/\partial x$ is the chemical potential of the C^{IV} constituent measured with respect to the average chemical potential of A^{III} and B^{V}. In fact, *any* incipient phase

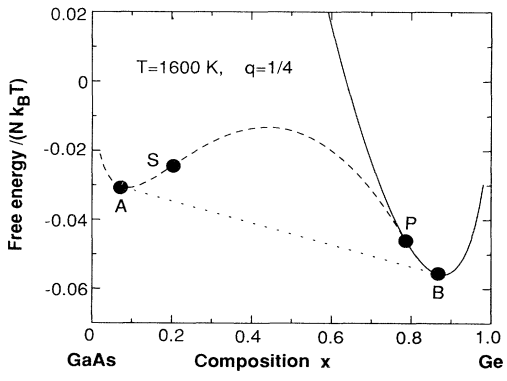

FIG. 10. Representative free energy vs composition curve of $(GaAs)_{1-x}Ge_{2x}$ for a temperature below the tricritical point. The dashed and solid lines indicate the zinc-blende and diamond phases, respectively. Points A and B are the limits of phase separation (represented by the dotted line), S is the zinc-blende phase spinodal, and P is the unstable second-order transition.

separation lowers the free energy in this regime.[85] (b) The dotted line in Figs. 8 and 9 from $(x,T)=(1,0)$ to (x_{tc},T_{tc}) is the *unstable* continuation of the second-order phase transition, which corresponds to point P in Fig. 10. The ZB solution immediately to the left of point P is thermodynamically unstable ($\partial\mu/\partial x<0$) with respect to long-range perturbations. Similar phase-transition lines have been called "metastable" in previous works[23,47] with the provision that long-range atomic interchanges are disallowed. Even then, the transition occurs only very close to $x=1$ at solid-state temperatures, contrary to experiment.

D. Results for compensated alloys

The effects of charge transfer on the phase diagrams are indicated in Figs. 8(b) and 9(b). It is clear that the main features (i), (ii), and (iii) of Sec. VI C still hold. The main change in the phase diagram is a scaling of the tricritical temperature by a ratio of approximately $J(q=\frac{1}{4})/\delta$. The decrease in the $\Delta Z_v=\pm 1$ bond energy produced by charge transfer therefore decreases the area of phase separation in the phase diagrams. A second, more subtle, change is a slight decrease in the tricritical concentration [from 0.727 in the $q=0$ case for both alloys to 0.688 in $(GaP)_{1-x}Si_{2x}$ and 0.692 in $(GaAs)_{1-x}Ge_{2x}$, both for $q=\frac{1}{4}$]. This latter effect is a direct consequence of interbond Madelung interactions. As discussed in Sec. V, the excess Madelung energy is larger in the ZB phase than in the D phase, due to the presence of a larger number of III-IV-III and V-IV-V clusters, which have positive nearest-neighbor-bond repulsions, in the former phase. Madelung energy, therefore, increases the region of stability of the D phase, displacing the tricritical concentration to lower values. These changes, however, are not sufficient to produce a significant modification of the phase diagrams at temperatures below the melting points of the constituents.

The positive values of the $\Delta Z_v=\pm 1$ bond energies[27,29,58,59] imply that phase separation between the usual zinc-blende (ZB) and diamond (D) structures is the equilibrium state at low temperatures, in agreement with the known[3] near mutual insolubility of $A^{III}B^{V}$ and C^{IV}. It might be thought, however, that new ordered structures could be stabilized if strong first-neighbor interbond electrostatic interactions, in excess of what the dielectric-constant approximation would grant, are introduced. One might try to increase the number of negative-energy contributions from first-neighbor pairs of bonds by placing the C^{IV} atoms on one fcc sublattice and the A^{III} and B^{V} atoms on the other in an "antiferromagnetic" configuration. However, this procedure leads to frustration effects on the triangular planes of the latter sublattice, so no new minimum-energy ordered configurations are produced.

It is possible also that metastable configurations, corresponding to local minima of the free energy with respect to the correlation functions, could explain the appearance of structures not found in equilibrium phase diagrams. However, no metastable single-phase states are found in the alloys at solid-state temperatures. As in the results

for the uncompensated case, we find that in the CVM pair approximation single phases are unstable in most of the phase-separation region, i.e., between the ZB spinodal and the unstable phase-transition curves. Furthermore, below melting temperatures [in $(GaAs)_{1-x}Ge_{2x}$ the eutectic temperature[79] is around 1140 K] the (unstable) continuous phase transition occurs only very close to $x=1$. These results lead us to conclude that 3D bulk lattice thermodynamics is unlikely to explain the existence of ZB or D single-phase $(A^{III}B^{V})_{1-x}C_{2x}^{IV}$ alloys, prepared at temperatures below 800 K and covering the whole composition range, as observed experimentally.

Of course, a large number of configurations (including superlattices) intermediate in energy between phase-separated and single-phase alloys can be designed by placing arbitrarily sized domains of pure (or nearly pure) constituents in arrangements where most of the $\Delta Z_v=\pm 1$ bonds occur in the domain walls. High diffusion barriers in the bulk imply that many of these structures are metastable in a broader sense than considered in the previous discussion, i.e., they are likely to be local minima of the free energy in a configurational space constituted by *all* continuous degrees of freedom of the system. *Lattice* statistical models, however, independently of the mathematical approximations used, are unable to describe this type of metastability.

The phase diagrams discussed in this section correspond to the Hamiltonian of Eq. (12) with

$$E_{\text{pair}}(q)=(N_D+N_A)J(q)$$

and $q=\frac{1}{4}$; the value of $J(q)$ was extracted from first-principles pseudopotential total-energy calculations for the superlattices with $x=\frac{1}{2}$. The model energies for $(GaP)_n/(Si_2)_n$ superlattices have a standard deviation of 17 meV per $\Delta Z_v=\pm 1$ bond with respect to the first-principles calculations at $x=\frac{1}{2}$ (see Table II). This fit does not use the data at $x=\frac{1}{8}$ and $\frac{7}{8}$. We can, however, use this model to *predict* the energies of the $x=\frac{1}{8}$ and $x=\frac{7}{8}$ ordered structures in $(GaP)_{1-x}Si_{2x}$. The predicted excess energies are, on average, 24 meV per $\Delta Z_v=\pm 1$ bond smaller than the pseudopotential results. This error—not significantly larger than the standard deviation for the $x=\frac{1}{2}$ fit—does not constitute sufficient evidence for introducing a concentration dependence into $J(q)$. If, however, we insist on reproducing the pseudopotential results for $x=\frac{1}{8}$ and $\frac{7}{8}$ by introducing a (say, parabolic) x dependence in $J(q)$, we find, in a phase diagram calculated with such a $J(q,x)$, a zinc-blende eutectic and, at lower temperatures, zinc-blende metastable solutions in the phase-separation regime. The metastable zinc-blende solutions are centered [like the minimum in $J(q,x)$] around $x=\frac{1}{2}$ and disappear for $T<1300$ K. At lower temperatures, the composition range where phase separation exists *increases* with respect to the concentration-independent $J(q)$ results. Our conclusions, therefore, are not affected.

Better statistical approximations should lower characteristic temperatures in the phase diagram, but are not expected to change its topology. As discussed in the Introduction, the CVM pair approximation results in an adequate description of the diamond lattice. The error of 6.7% in the prediction of the spin-$\frac{1}{2}$ Ising-model critical temperature is within the accuracy of the parameters in our Hamiltonian.

VII. CONCLUSIONS

In this work we have analyzed the consequences of a quantitative energy model of $(A^{III}B^{V})_n/(C_2^{IV})_n$ superlattices on the excess energy and thermodynamic properties of $(A^{III}B^{V})_{1-x}C_{2x}^{IV}$ alloys. The model incorporates the effects of charge transfer between donor and acceptor bonds. The following conclusions are drawn.

(i) Charge transfer between donor and acceptor bonds acts to make both nonisovalent superlattices and nonisovalent alloys less unstable.

(ii) The different contributions to the excess enthalpy of nonisovalent alloys have been identified. It has been established that charge transfer acts to stabilize the diamond phase with respect to the zinc-blende phase.

(iii) Equilibrium phase diagrams in the pair approximation of the cluster-variation method show that, although characteristic temperatures have been lowered and the regime of stability of the diamond phase has been increased by charge-transfer mechanisms, phase separation is still the stable thermodynamic state of the 3D bulk system at temperatures below the melting point. This conclusion is independent of the presence or absence of A^{III}-A^{III} and B^{V}-B^{V} bonds in the model. The single-phase zinc-blende and diamond structures are both unstable in most of the composition range at solid-state temperatures.

The main limitations of our approach are (i) simplifications used in the energy model, such as the use of concentration-independent interaction energies, and (ii) the use of the CVM pair statistical approximation. Although details of the phase diagram could be changed if a more accurate description were available, as discussed in Sec. VI, phase separation at typical preparation temperatures will continue to be the only thermodynamically stable solution.

The failure of a *three-dimensional bulk* thermodynamic model opens the possibility that a *two-dimensional surface* model might be appropriate. Solid solutions of $(A^{III}B^{V})_{1-x}C_{2x}^{IV}$ alloys produced by epitaxial-growth techniques could correspond to metastable surface configurations, where the atoms are allowed to find minimum-energy positions on the free surface during the growth process, but have essentially zero diffusion when covered. Recent studies of such models for isovalent alloys by Froyen and Zunger[51] have shown that *surface reconstruction* (neglected in growth models) acts to select minimum-energy configurations that are absent in 3D thermodynamic models, but are observed experimentally. This mechanism differs from the growth models used previously[43–45] since the latter have not allowed for surface diffusion and have not been based on direct energy considerations for the sticking probabilities of different species.

ACKNOWLEDGMENTS

We thank R. G. Dandrea for useful discussions and for the results of Ref. 67. This work was supported in part by the U.S. Department of Energy, Office of Energy Research, Basic Energy Science, Grant No. DE-AC02-77-CH00178. One of us (R.O.) would like to thank Coordenação de Aperfeiçoamento de Pessoal de Nível Superior (Brazil) for support.

APPENDIX A: SUPERPOSITION APPROXIMATIONS

To introduce interactions beyond the size of the basic cluster (in this case, the nearest-neighbor pair), we use mean-field-like "superposition approximations,"[75–77] that would be exact if there were only one path between two points of the lattice (as in one-dimensional systems or Bethe lattices). For the finite-range energy expression of Eq. (13), we use the probabilities of occupation of first-neighbor bond pairs,

$$p^{(1)}_{(ij)(jk)}=\frac{1}{2}\left[\frac{y_{ij}y_{kj}}{x_j^{\beta}}+\frac{y_{ji}y_{jk}}{x_j^{\alpha}}\right], \tag{A1}$$

second-neighbor bond pairs,

$$p^{(2)}_{(ij)(kl)}=\frac{y_{ij}y_{kj}y_{kl}}{x_j^{\beta}x_k^{\alpha}}, \tag{A2}$$

third-neighbor bond pairs along zigzag chains,

$$p^{(3z)}_{(ij)(kl)}=p^{(2)}_{(ij)(kl)}, \tag{A3}$$

and third-neighbor bond pairs in the same hexagon,

$$p^{(3h)}_{(ij)(lm)}=\frac{1}{2}\left[\sum_k\frac{y_{ij}y_{kj}y_{kl}y_{ml}}{x_j^{\beta}x_k^{\alpha}x_l^{\beta}}+\sum_k\frac{y_{ji}y_{jk}y_{lk}y_{lm}}{x_j^{\alpha}x_k^{\beta}x_l^{\alpha}}\right]. \tag{A4}$$

The superposition approximations are the same for second-neighbor bond pairs and for third-neighbor bond pairs along zigzag chains due to the local topological equivalence of the two four-site clusters (see Fig. 4). The two terms on the right-hand side of Eqs. (A1) and (A4) indicate the two possible sublattice locations of the corresponding clusters.

APPENDIX B: ISOMORPHISM OF THE ALLOY HAMILTONIAN WITH THE BLUME-EMERY-GRIFFITHS MODEL

The most general Hamiltonian for a spin-1 Ising model that includes only site energies and nearest-neighbor interactions has the form[80]

$$\mathcal{H}_{\rm BEG}=-J\sum_{(ij)}S_iS_j-K\sum_{(ij)}S_i^2S_j^2-L\sum_{(ij)}(S_i^2S_j+S_iS_j^2)+D\sum_i S_i^2-H\sum_i S_i, \tag{B1}$$

where the indices (ij) indicate sums over nearest-neighbor pairs of sites. The terms containing J, K, and D constitute the original Blume-Emery-Griffiths (BEG) Hamiltonian,[52] used to model tricritical behavior in He^3-He^4 mixtures. In terms of the correlation functions defined by Eq. (26), we can write

$$\mathcal{H}_{\rm BEG}=\frac{Nz}{2}[-J\xi_5-K\xi_6-L(\xi_7+\xi_8)]+\frac{N}{2}[D(\xi_3+\xi_4)-H(\xi_1+\xi_2)], \tag{B2}$$

where $z=4$ is the lattice coordination number.

An isomorphism exists between the complete BEG Hamiltonian of Eq. (B1) and the three-species alloy problem with only nearest-neighbor interactions (to which our model without charge transfer corresponds). The alloy Hamiltonian can be expressed in terms of pairwise interatomic energies (ε_{kl}) and chemical potentials (μ_k) as

$$\mathcal{H}_{\rm alloy}=\frac{Nz}{2}\sum_{k,l}\varepsilon_{kl}y_{kl}-\frac{N}{2}\sum_k\mu_k(x_k^{\alpha}+x_k^{\beta}), \tag{B3}$$

where k and l indicate the different atomic species. The "spin-1 cluster algebra"[78] can then be used to express the cluster probabilities $\{y_{kl}\}$ and $\{x_k\}$ in terms of the correlation functions $\{\xi_n\}$. Comparison of coefficients of each ξ_n then establishes the following correspondence between the energy parameters of $\mathcal{H}_{\rm BEG}$ and $\mathcal{H}_{\rm alloy}$,[81] with the notation $+,-,0$ for elements $A^{\rm III}$, $B^{\rm V}$, and $C^{\rm IV}$:

$$\begin{aligned}
J&=-W/2,\\
K&=-W/2+2\delta,\\
L&=(-\tfrac{1}{4})(\varepsilon_{++}-\varepsilon_{--}-2\varepsilon_{+0}+2\varepsilon_{-0}),\\
D&=\Delta\mu-z\varepsilon_{00}+(z/2)(\varepsilon_{+0}+\varepsilon_{-0}),\\
H&=\tfrac{1}{2}(\mu_+-\mu_-)-(z/2)(\varepsilon_{+0}-\varepsilon_{-0}),
\end{aligned} \tag{B4}$$

where δ is the $\Delta Z_v=\pm1$ bond energy [Eq. (2)], W is the $\Delta Z_v=\pm2$ bond energy, given by

$$W=\tfrac{1}{2}(\varepsilon_{++}+\varepsilon_{--}-2\varepsilon_{+-}), \tag{B5}$$

and $\Delta\mu$ is the chemical potential difference

$$\Delta\mu=\mu_0-\tfrac{1}{2}(\mu_++\mu_-). \tag{B6}$$

The restrictions of no $\Delta Z_v=\pm2$ bonds (or $W\to\infty$) [Eq. (27)] and of equal concentrations of $+$ and $-$ spins [Eq. (28)] reduce the BEG Hamiltonian to

$$\mathcal{H}=\frac{Nz}{2}(K-J)\xi_5+\frac{N}{2}D(\xi_3+\xi_4), \tag{B7}$$

where $K-J=2\delta$. The parameter D controls the concentration x of spins 0. For a fixed x, the $\Delta Z_v=\pm1$ bond energy δ is the only relevant energy parameter.

We finally give an argument for the absence of sublattice ordering for spins 0 [Eq. (29)]. In fact, this type of sublattice "quadrupolar" (SQ) ordering occurs in the BEG model for a certain range of values of the energy parameters.[82,83] In our case, the effective Ising-like interac-

tion is antiferromagnetic ($J<0$). The condition for appearance of SQ ordering is then[83]

$$K+|J|<D/z<0 . \tag{B8}$$

However, we have in the present problem $K+|J|=K-J=2\delta>0$. It is safe, therefore, to assume $\xi_3=\xi_4$ and reduce the number of independent correlation functions to three [Eq. (30)].

*Permanent address: Departamento de Física, Universidade de Brasília, 70910 Brasília, Distrito Federal, Brazil.

[1]J. E. Greene, J. Vac. Sci. Technol. B **1**, 229 (1983).
[2]S. A. Barnett, B. Kramer, L. T. Romano, S. I. Shah, M. A. Ray, S. Fang, and J. E. Greene, in *Layered Structures, Epitaxy, and Interfaces,* Proceedings of the Materials Research Society Symposium, edited by J. M. Gibson and L. R. Dawson (Materials Research Society, Pittsburgh, 1985), Vol. 37, p. 285.
[3]*Landolt-Börnstein Relationships in Science and Technology,* New Series, Vol. III/17a, edited by O. Madelung, M. Schulz, and H. Weiss (Springer, Berlin, 1987).
[4]See discussion in E. Parthé, *Crystal Chemistry of Tetrahedral Structures* (Gordon and Breach, New York, 1965), p. 5.
[5]A. J. Noreika and M. H. Francombe, J. Appl. Phys. **45**, 3690 (1974).
[6]K. C. Cadien, A. H. Eltoukhy, and J. E. Greene, Appl. Phys. Lett. **38**, 773 (1981).
[7]S. A. Barnett, M. A. Ray, A. Lastras, B. Kramer, J. E. Greene, P. M. Raccah, and L. L. Abels, Electron. Lett. **18**, 891 (1982).
[8]Zh. I. Alferov, M. Z. Zhingarev, S. G. Khonnikov, I. I. Mokan, V. P. Ulin, V. E. Umanskiĭ, and B. S. Yavich, Fiz. Tekh. Poluprovodn. **16**, 831 (1982) [Sov. Phys.—Semicond. **16**, 532 (1982)].
[9]L. Romano, J. -E. Sundgren, S. A. Barnett, and J. E. Greene, Superlatt. Microstruct. **2**, 233 (1986).
[10]S. I. Shah, J. E. Greene, L. L. Abels and P. M. Raccah, J. Cryst. Growth **91**, 71 (1988).
[11]I. Banerjee, D. W. Chung, and H. Kroemer, Appl. Phys. Lett. **46**, 494 (1985).
[12]M. Glicksman and W. D. Kraeft, Solid State Electron. **28**, 151 (1985).
[13]T. N. Krabach, N. Wada, M. V. Klein, K. C. Cadien, and J. E. Greene, Solid State Commun. **45**, 895 (1983).
[14]R. Beserman, J. E. Greene, M. V. Klein, T. N. Krabach, T. C. McGlinn, L. T. Romano, and S. I. Shah, in *Proceedings of the Seventeenth International Conference on the Physics of Semiconductors,* edited by J. D. Chadi and W. A. Harrison (Springer, New York, 1985), p. 961.
[15]T. C. McGlinn, M. V. Klein, L. T. Romano, and J. E. Greene, Phys. Rev. B **38**, 3362 (1988).
[16]K. C. Cadien, B. C. Muddle, and J. E. Greene, J. Appl. Phys. **55**, 4177 (1984).
[17]E. A. Stern, F. Ellis, K. Kim, L. Romano, S. I. Shah, and J. E. Greene, Phys. Rev. Lett. **54**, 905 (1985).
[18]S. I. Shah, B. Kramer, S. A. Barnett, and J. E. Greene, J. Appl. Phys. **59**, 1482 (1986).
[19]L. T. Romano, I. M. Robertson, J. E. Greene, and J. E. Sundgren, Phys. Rev. B **36**, 7523 (1987).
[20]D. H. Mei, Y. -W. Kim, D. Lubben, I. M. Robertson, and J. E. Greene, Appl. Phys. Lett. **55**, 2649 (1989).
[21]A. D. F. Kahn, J. A. Eades, L. T. Romano, S. I. Shah, and J. E. Greene, Phys. Rev. Lett. **58**, 682 (1987).
[22]K. E. Newman, A. Lastras-Martinez, B. Kramer, S. A. Barnet, M. A. Ray, J. D. Dow, J. E. Greene, and P. M. Raccah, Phys. Rev. Lett. **50**, 1466 (1983).
[23]K. E. Newman and J. D. Dow, Phys. Rev. B **27**, 7495 (1983).
[24]K. E. Newman, J. D. Dow, B. A. Bunker, L. L. Abels, P. M. Raccah, S. Ugur, D. Z. Xue, and A. Kobayashi, Phys. Rev. B **39**, 657 (1989).
[25]S. Ciraci, in *Band Structure Engineering in Semiconductor Microstructures,* edited by R. A. Abram and M. Jaros (Plenum, New York, 1989), p. 33.
[26]D. M. Bylander and L. Kleinman, Phys. Rev. B **39**, 5166 (1989); **41**, 3509 (1990).
[27]S. Lee, D. M. Bylander, and L. Kleinman, Phys. Rev. B **41**, 10 264 (1990).
[28]T. Ohno, Solid State Commun. **74**, 7 (1990).
[29]R. G. Dandrea, S. Froyen, and A. Zunger, Phys. Rev. B **42**, 3213 (1990).
[30]C. G. van de Walle and R. M. Martin, J. Vac. Sci. Technol. B **4**, 1055 (1986).
[31]M. Cardona and N. E. Christensen, Phys. Rev. B **35**, 6182 (1987).
[32]J. Tersoff, in *Heterojunction Band Discontinuities: Physics and Device Applications,* edited by F. Capasso and G. Margaritondo (North-Holland, Amsterdam, 1987), p. 3.
[33]P. A. Sterne and C. S. Wang, Phys. Rev. B **37**, 10 436 (1988).
[34]E. Kaxiras, O. L. Alerhand, J. D. Joannopolous, and G. W. Turner, Phys. Rev. Lett. **62**, 2484 (1989).
[35]J. E. Northrup, Phys. Rev. Lett. **62**, 2487 (1989).
[36]W. A. Harrison and E. A. Kraut, Phys. Rev. B **37**, 8244 (1988).
[37]J. E. Fischer, M. Glicksman, and J. A. Van Vechten, in *Physics of Semiconductors,* Proceedings of the Thirteenth International Conference, edited by F. G. Fumi (North-Holland, Amsterdam, 1976), p. 541.
[38]D. Stauffer, Phys. Rep. **54**, 1 (1979).
[39]R. Zallen, *The Physics of Amorphous Solids* (Wiley, New York, 1983), Chap. 4.
[40]M. I. D'yakonov and M. É. Raĭkh, Fiz. Tekh. Poluprovodn. **16**, 890 (1982) [Sov. Phys.—Semicond. **16**, 570 (1982)].
[41]H. Holloway and L. C. Davis, Phys. Rev. Lett. **53**, 830 (1984); **53**, 1510(E) (1984).
[42]H. Holloway, Phys. Rev. B **37**, 874 (1988).
[43]K. Kim and E. A. Stern, Phys. Rev. B **32**, 1019 (1985).
[44]L. C. Davis and H. Holloway, Solid State Commun. **64**, 121 (1987); Phys Rev. B **35**, 2767 (1987); **38**, 4294 (1988); H. Holloway and L. C. Davis, *ibid.* **35**, 3823 (1987).
[45]G. F. Preger, C. M. Chaves, and B. Koiller, Phys. Rev. B **38**, 13 447 (1988); R. B. Capaz, G. F. Preger, and B. Koiller, *ibid.* **40**, 8299 (1989).
[46]B. Koiller, M. A. Davidovich, and R. Osório, Solid State Commun. **5**, 861 (1985).
[47]B. -L. Gu, K. E. Newman, and P. A. Fedders, Phys. Rev. B **35**, 9135 (1987).
[48]W. L. Bragg and E. J. Williams, Proc. R. Soc. London Ser. A **145**, 699 (1934).
[49]R. Kikuchi, Phys. Rev. **81**, 988 (1951).
[50]See, for instance, K. Binder and D. W. Heerman, *Monte Carlo Simulations in Statistical Physics* (Springer, Berlin, 1988).
[51]S. Matsumura, N. Kuwano, and K. Oki, Jpn. J. Appl. Phys. **29**, 688 (1990), give a formal description of surface ground states in isovalent (III-V)/(III-V) alloys. S. Froyen and A.

Zunger, Phys. Rev. Lett. **66**, 2132 (1991), demonstrated by total-energy calculations that the energy-minimizing surface geometry of $Ga_{0.5}In_{0.5}P$ is identical to the one observed after growth but differs from the bulk-stable geometry. See also a preliminary report in J. E. Bernard, R. G. Dandrea, L. G. Ferreira, S. Froyen, S.-H. Wei, and A. Zunger, Appl. Phys. Lett. **56**, 731 (1990).

[52]M. Blume, V. J. Emery, and R. B. Griffiths, Phys. Rev. A **4**, 1071 (1971).

[53]K. C. Hass and R. J. Baird, Phys. Rev. B **38**, 3591 (1988).

[54]Y. Bar-Yam, D. Kandel, and E. Domany, Phys. Rev. B **41**, 12 869 (1990).

[55]S. Wolfram, Rev. Mod. Phys. **55**, 601 (1983).

[56]I. G. Enting, J. Phys. C **10**, 1379 (1977).

[57]E. Domany and W. Kinzel, Phys. Rev. Lett. **53**, 311 (1984).

[58]M. A. Davidovich, B. Koiller, R. Osório, and M. O. Robbins, Phys. Rev. B **38**, 10 524 (1988).

[59]T. Ito, Jpn. J. Appl. Phys. **26**, L1177 (1987); **27**, 1916 (1988).

[60]W. Kohn and L. J. Sham, Phys. Rev. A **140**, 1133 (1965).

[61]J. Ihm, A. Zunger, and M. L. Cohen, J. Phys. C **12**, 4409 (1979).

[62]G. A. Baraff and M. Schlüter, Phys. Rev. B **33**, 7346 (1986).

[63]M. Kurata, R. Kikuchi, and T. Watari, J. Chem. Phys. **21**, 434 (1953).

[64]J. W. Essam and M. F. Sykes, Physica (Utrecht) **29**, 378 (1963).

[65]See, for instance, L. E. Reichl, *A Modern Course in Statistical Physics* (University of Texas, Austin, 1980), Chap. 2.

[66]For a review, see M. Tosi, in *Solid State Physics,* edited by F. Seitz and D. Turnbull (Academic, New York, 1964), Vol. 16, p. 1.

[67]R. G. Dandrea (private communication).

[68]W. A. Harrison, Phys. Rev. B **27**, 3592 (1983).

[69]The ejected Ga and P atoms are assumed to be at the surface; this does not alter the energy since these two new surface atoms also convert, on average, two previous surface atoms into "bulk" atoms.

[70]It is more appropriate to use this average instead of the individual heats of solution as a prediction of the model since by assigning the compensated charge to the midpoint of a $\Delta Z_v = \pm 1$ bond, the model does not distinguish, for example, the energy of a cluster where a Ga atom is surrounded by four Si atoms from that where a Si atom is surrounded by four Ga atoms.

[71]The cluster–Bethe-lattice calculation gives a $\Delta Z_v = \pm 1$ bond energy $\delta = 0.15$ eV. Since no charge-transfer effects are present in that model, defect energies are given by our Eqs. (16) and (18). Note that the values quoted in Ref. 58 as the Kraut-Harrison values for the sum of *bound* pairs in GaAs/Ge, correspond, in fact, to *unbound* pairs.

[72]Previous UPTB data agree well with Ref. 36 for the case of lattice-matched systems: E. A. Kraut and W. A. Harrison, J. Vac. Sci. Technol. B **2**, 409 (1984); **3**, 1267 (1985).

[73]The percolation problem is usually associated with the zero-temperature limit of dilute Ising models. See, e.g., R. B. Stinchcombe, in *Phase Transitions and Critical Phenomena,* edited by C. Domb and J. L. Lebowitz (Academic, London, 1983), Vol. 7, Chap. 3. In the present case, our maximum-entropy structures correspond to the *infinite-* temperature limit of the short-range model with no $\Delta Z_v = \pm 2$ bonds, but it is still a zero-temperature limit for a model where *only* $\Delta Z_v = \pm 2$ bond energies are nonzero. In other words, we are treating a regime where $k_B T$ is intermediate between the energies of $\Delta Z_v = \pm 1$ bonds and the energies of $\Delta Z_v = \pm 2$ bonds.

[74]R. Kikuchi, J. Phys. (Paris) Colloq. **38**, C7-307 (1977).

[75]R. Kikuchi, J. Chem. Phys. **19**, 1230 (1951).

[76]T. Morita, J. Phys. Soc. Jpn. **12**, 753 (1957).

[77]R. Osório and B. Koiller, Physica A **131**, 263 (1985).

[78]P. R. C. Holvorcem and R. Osório, Physica A **152**, 431 (1988).

[79]Y. Takada, T. Hirai, and M. Hirao, J. Electrochem. Soc. **112**, 363 (1965).

[80]D. Mukamel and M. Blume, Phys. Rev. A **10**, 610 (1974).

[81]Our equations correct some of the signs in Eq. (10) of Ref. 80 and the coefficient for $(E_{13}+E_{23})$ in Eq. (5c) of Ref. 47. The D and H terms are missing in Ref. 47.

[82]M. Tanaka and T. Kawabe, J. Phys. Soc. Jpn. **54**, 2194 (1985).

[83]R. Osório, M. J. de Oliveira, and S. R. Salinas, J. Phys. Condens. Matt. **1**, 6887 (1989).

[84]In Ref. 47, Gu *et al.* stated that "the problem is determined only by two parameters," namely, $t = k_B T/|\varepsilon_{\mathrm{III-V}}|$ and $R = (\varepsilon_{\mathrm{IV-IV}} - \varepsilon_{\mathrm{III-IV}} - \varepsilon_{\mathrm{IV-V}})/\varepsilon_{\mathrm{III-V}}$. In fact, $k_B T/\delta$ (in our notation) is the *only* relevant parameter. [Our $\Delta Z_v = \pm 1$ bond energy δ can be expressed in terms of Gu *et al.*'s notation as $\delta = (R+1)\varepsilon_{\mathrm{III-V}}/2$.] It is easily verified that the four phase diagrams presented in Fig. 6 of Ref. 47 are equivalent under appropriate scalings of the temperature axis.

[85]A discussion of stability analysis and spinodal decomposition is given by D. de Fontaine, in *Solid State Physics,* edited by H. Ehrenreich, F. Seitz and D. Turnbull (Academic, New York, 1977), Vol. 34, p. 73.